Aerosol liquid water promotes the formation of water-soluble organic nitrogen in submicrometer aerosols in a suburban forest

Yu Xu,[†] Yuzo Miyazaki,*[,†] Eri Tachibana,[†] Kei Sato,[‡] Sathiyamurthi Ramasamy,[‡, §] Tomoki Mochizuki,[†, ▽] Yasuhiro Sadanaga,[∥] Yoshihiro Nakashima,[⊥] Yosuke Sakamoto,[‡, §, #] Kazuhide Matsuda,[⊥] and Yoshizumi Kajii[‡, §, #]

[†]Institute of Low Temperature Science, Hokkaido University, Sapporo 060-0819, Japan

[‡]National Institute for Environmental Studies, Onogawa, Tsukuba, Ibaraki 305-5506, Japan

[§]Graduate School of Global Environmental Studies, Kyoto University, Nihonmatsucho, Sakyo-ku, Kyoto 606-8501, Japan

[∥]Department of Applied Chemistry, Osaka Prefecture University, Sakai 599-8531, Japan

[⊥]Department of Environmental Science on Biosphere, Tokyo University of Agriculture and Technology, Tokyo 183-8509, Japan

[#]Graduate School of Human and Environmental Studies, Kyoto University, Nihonmatsucho, Sakyo-ku, Kyoto 606-8501, Japan

*Corresponding author e-mail: yuzom@lowtem.hokudai.ac.jp

Phone: +81-11-706-7448 Address: Institute of Low Temperature Science, Hokkaido University, Sapporo 060-0819, Japan

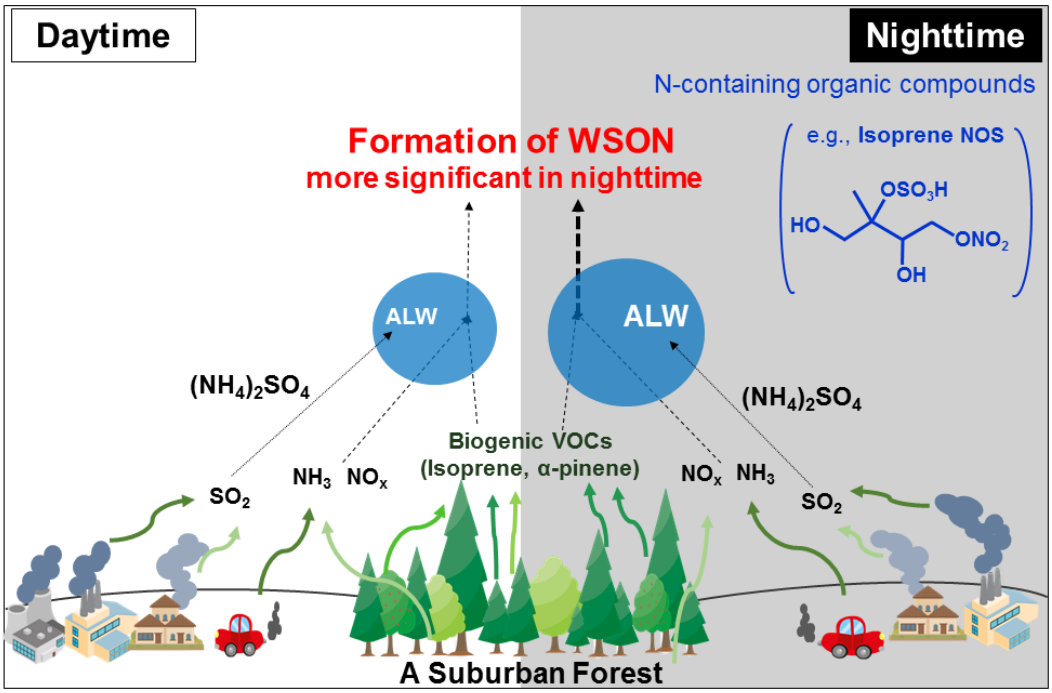
Daytime
Nighttime
N-containing organic compounds
Formation of WSON
more significant in nighttime
e.g., Isoprene NOS
OSO3H
HO
ONO2
OH
ALW
ALW
(NH4)2SO4
(NH4)2SO4
Biogenic VOCs
(Isoprene, α-pinene)
SO2
NH3
NOx
NOx
NH3
SO2
A Suburban Forest

ABSTACT: Water-soluble organic nitrogen (WSON) affects the formation, chemical transformations, hygroscopicity, and acidity of organic aerosols as well as biogeochemical cycles of nitrogen. However, large uncertainties exist in the origins and formation processes of WSON. Submicrometer aerosol particles were collected at a suburban forest site in Tokyo in summer 2015 to investigate relative impacts of anthropogenic and biogenic sources on WSON formations and their linkages with aerosol liquid water (ALW). The concentrations of WSON (ave. 225 ± 100 ngN m^{-3}) and ALW exhibited peaks during nighttime, which showed a significant positive correlation, suggesting that ALW significantly contributed to WSON formation. Further, the thermodynamic predictions by ISORROPIA-II suggest that ALW was primarily driven by anthropogenic sulfate. Our analysis, including positive matrix factorization, suggests that aqueous-phase reactions of ammonium and reactive nitrogen with biogenic volatile organic compounds (VOCs) play a key role in WSON formation in submicrometer particles, which is particularly significant in nighttime, at the suburban forest site. The formation of WSON associated with biogenic VOCs and ALW was partly supported by the molecular characterization of WSON. The overall result suggests that ALW is an important driver for the formation of aerosol WSON through a combination of anthropogenic and biogenic sources.

■ INTRODUCTION.

Water-soluble organic nitrogen (WSON) typically accounts for up to ~30% of water-soluble total nitrogen by mass in atmospheric aerosols.[1-4] WSON can affect water-solubility, acidity, and hygroscopicity of aerosol particles,[3, 5, 6] which are closely linked with air quality and climate-relevant factors such as cloud formation. Moreover, the atmospheric deposition of WSON onto terrestrial and marine environments affects the structure and function of natural ecosystems, such as eutrophication and changes in biodiversity.[5, 7-10] Therefore, it is of great importance to understand the origins and formation processes of WSON in aerosols.

WSON in atmospheric aerosols can be associated with primary emissions from terrestrial vegetation such as fragments of plants, bacteria, fungi, and pollen.[1, 3, 11] In addition, secondary formation is also a possible source of WSON, which includes reactions of biogenic volatile organic compounds (VOCs), such as monoterpenes and isoprene, with reactive nitrogen.[12-14] A laboratory chamber experiment conducted by Surratt et al.[15] reported that the oxidation of isoprene with nitrogen oxide (NO_x) results in the formation of methacryloyl peroxynitrate (MPAN)-derived ON in particle phase. Other laboratory experiments have demonstrated the production of nitrooxy organosulfates (NOSs) and other organic nitrates (e.g., dihydroxynitrates and monohydroxynitrates) through reactions of α-/β-pinene and NO_x.[14, 16, 17, 18] Furthermore, glyoxal monomers can react with ammonium (NH_4^+)/ammonia (NH_3) to form nitrogen-containing organic compounds (NOCs) in aqueous-phase particles or nanodroplets containing ammonium.[19, 20] Nevertheless, there are still substantial gaps in our current

knowledge on the sources and formation processes of WSON in ambient aerosols.

It has been recognized that aerosol liquid water (ALW) can significantly enhance secondary organic aerosol (SOA) mass yield.[21-25] This is because ALW not only facilitates partitioning of gas-phase water-soluble organic matter into the particle phase but also provides a medium for aqueous reactions to form SOA.[21, 23, 26] Previous studies have reported that the amount of ALW is closely associated with local ambient conditions, such as relative humidity (RH) and aerosol mass of chemical components (e.g., sulfate or nitrate).[22, 25, 27-29] In general, forest environments have potentially high RH and larger emissions of water-soluble precursors of biogenic SOA compared to urban environments.[30] In addition, a forest region influenced by anthropogenic air masses with high NO_x concentrations is expected to promote SOA associated with ALW.[31, 32] A recent field study conducted at a cool-temperate forest site suggested that biogenic SOA and primary biological aerosol particles (PBAPs) accounted for substantial fractions of the submicrometer water-soluble organic carbon (WSOC) aerosols by mass.[33] Despite WSON being an important compound class of WSOC, the potential roles of ALW in the formation of WSON aerosols, particularly in the forest atmosphere, are not well-documented.

In this study, we present the ambient measurements of the concentrations of WSON, the predicted ALW, and the relevant chemical parameters in submicrometer aerosol particles collected at a suburban forest site in Tokyo in summer 2015. The aims of the study are (1) to investigate the origins of ALW and WSON in the aerosols at the forest site, (2) to elucidate the role of ALW in WSON formation, and (3) to investigate

the potential formation processes for WSON with a focus on the relative impacts of anthropogenic and biogenic sources.

■ EXPERIMENTAL SECTION

Site Description. Intensive measurements of aerosol and gas species were performed from July 23 to August 8 in 2015 at the Field Museum Tama Hill (FM-Tama, 35.6385°N, 139.3781°E) measurement station of Tokyo University of Agriculture and Technology.[34, 35, 36] The site is located approximately 30 km west of center of Tokyo, Japan (**Figure S1a**). The dominant species of the trees at the forest site are *Quercus serrata* (Japanese konara oak), *Quercus acutissima* (sawtooths oak), and *Cryptomeria japonica* (Japanese cedar). The biogenic emissions of VOCs and aerosols have been previously reported for this forest site.[34] Because the forest site is characterized as a typical suburban forest area, the site is also expected to be influenced by anthropogenic air masses transported from the urban area.[36]

Meteorological parameters, including local wind speeds and wind directions, amount of rainfall, RH, ambient temperature, and photosynthetically active radiation (PAR), were monitored at the site. The local wind speeds were mostly < 5 m s^{-1} during the study period (**Figures S1b** and **S2a**), indicating that most of the observed aerosols were affected by emission sources in the forest area. However, the wind speeds sometimes exceeded 5 m s^{-1}, particularly in daytime when the southerly winds were predominantly observed, suggesting that the observed air masses were mostly transported from the south directions of the urban area during the daytime. This

suggests that the forest site was also influenced by anthropogenic air masses in addition to the local biogenic sources, particularly in daytime. Only four rainfall events occurred during the entire sampling period (**Figure S2**), indicating that the removal of atmospheric components by rainfall is likely insignificant in this study.

Aerosol Sampling, Chemical Analysis, and Measurements of Gas Species. Submicrometer aerosol particles (with diameters of less than 0.95 μm) were continuously collected using a high-volume air sampler (HVAS; Model 120SL, Kimoto Electric, Osaka, Japan). A cascade impactor (CI; Series 230, Tisch Environmental, Cleves, OH, USA) was attached to HVAS, which collected submicrometer particles onto quartz fiber filters (25 cm × 20 cm) set on the bottom stage of CI. The duration of each aerosol sampling was approximately 3 h during daytime (9:00−18:00 LT) and approximately 15 h during nighttime (18:00−9:00 LT). The collected aerosol samples were stored individually in glass jars with a Teflon-lined screw top cap at −20 °C prior to the analysis.

For the determination of inorganic ions, a portion of each filter sample was extracted with ultrapure water (>18 MΩ cm^{-1}) using an ultrasonic bath. The extracts were then filtrated with a disc filter (Millex-GV, 0.22 μm, Millipore, Billerica, MA, USA). The mass concentrations of major inorganic ions, including sulfate, nitrate, and ammonium, were measured using an ion chromatograph (Model 761 compact IC; Metrohm).[37]

To determine the concentrations of WSOC and water-soluble total nitrogen (WSTN), another filter cut was extracted with ultrapure water. The extracts were

filtrated with the disc filter in the same way as above, and WSOC and WSTN concentrations were determined using a total organic carbon (TOC)/total nitrogen (TN) analyzer (Model TOC-Vcsh, Shimadzu).[38] In this study, the mass concentrations of WSOC were converted to those of water-soluble organic matter (WSOM) using a conversion factor of 1.8.[33, 39-41] The mass concentration of WSON is defined as the difference in the concentrations between WSTN and inorganic nitrogen (IN = NH_4^+_N + NO_3^-_N + NO_2^-_N), namely [WSON] = [WSTN] – [IN].

For the analysis of biogenic molecular tracer compounds, a filter portion was extracted with dichloromethane/methanol. The –COOH and –OH functional groups in the extracts were reacted with N,O-bis-(trimethylsilyl) trifluoroacetamide (BSTFA) to derive trimethylsilyl (TMS) esters and TMS ethers, respectively. The TMS derivatives were then analyzed for 2-methyltetrols, 3-methyl-1,2,3-butanetricarboxylic acid (3-MBTCA), pinic acid, pinonic acid, arabitol, mannitol, sucrose, and trehalose (**Table S1**) by using a capillary gas chromatograph (GC7890, Agilent, Santa Clara, CA, USA) coupled with a mass spectrometer (5973 MSD, Agilent, Santa Clara, CA, USA).[1]

To determine the concentrations of NOSs, another filter portion was extracted with methanol. Prior to the extraction, sodium ethyl sulfate-d5 was added to each filter sample as an internal standard. The extracted sample was injected into negative-mode electrospray ionization/liquid chromatography-mass spectrometry (ESI/LC-MS) (LC-MS-2020, Shimadzu).[42] In this study, we measured a molecular marker of isoprene-derived NOS detected at m/z 260 (isoprene NOS).[42] Sodium methyl sulfate was used as the surrogate standard for NOS, because it has been often used as a surrogate standard

for isoprene organosulfate.[43] It is noted that several chromatographic peaks were observed for the NOS of m/z 260, suggesting that several isomers are present for NOS. In the present study, the sum of these isomers was used to calculate the total concentrations of the NOS of m/z 260.

The mass concentrations of organic carbon (OC) and elemental carbon (EC) were measured using an OC/EC analyzer.[38] The concentrations of α-pinene and limonene were measured using a proton-transfer-reaction mass spectrometer (PTR-MS, IONICON).[34] Ambient measurements of ozone (O_3), carbon monoxide (CO), and NO_x (= NO + NO_2) concentrations were simultaneously performed using an ultraviolet absorption analyzer (Thermo Scientific, model 49C), a non-disperse infrared absorption analyzer (Thermo Scientific, model 48C), and a chemiluminescence analyzer (Thermo Scientific, model 42iTL).[34]

Predicting ALW using a Thermodynamic Model. To predict the mass concentration of ALW, we used a thermodynamic model, ISORROPIA-II,[27, 29] which calculates the ALW concentration with particle-phase concentrations of Na^+, SO_4^{2-}, NH_4^+, NO_3^-, Cl^-, Ca^{2+}, K^+, and Mg^{2+}, as well as meteorological conditions (RH and ambient temperature) as input. For our analysis, the inputs to ISORROPIA-II included the inorganic ions measured by IC as well as the RH and temperature monitored at the forest site (**Supporting Information (SI)**). To estimate the contributions of particle water associated with organic fractions to ALW, the organic hygroscopicity parameter was calculated (**SI**). ALW was calculated as the sum of water associated with individual aerosol chemical components (i.e., the sum of ions and lumped organics) based on the

Zdanovskii–Stokes–Robinson (ZSR) relationship.[29, 44, 45] The calculation assumed that the particles were internally mixed.

■ RESULTS AND DISCUSSION

Temporal Variations of Water-Soluble Components in Submicrometer Aerosol Particles. Figures 1a and **1b** show the time series of the mass fractions and concentrations of the major components of submicrometer water-soluble aerosols. On average, WSOM and sulfate were the dominant components, which accounted for 33 ± 11% and 49 ± 13% of the submicrometer water-soluble aerosols, respectively. Ammonium was the third most abundant chemical component, whose concentrations showed a temporal variation similar to that of sulfate (**Figure 1b**). During July 27 to August 3, the mass concentration levels and fractions of sulfate tended to increase, whereas those of WSOM (WSOC) showed an opposite trend. The mass fractions and concentrations of WSOC exhibited a distinct diurnal cycle, with a maximum in the morning until noontime and a minimum in the nighttime. A clear diurnal pattern was also observed for the sulfate concentrations, with peaks in the afternoon. These dissimilarities in the temporal variations of WSOM and sulfate suggested that the dominant sources differed between these two major components.

Figure 1c shows temporal variations in the concentrations of 2-methyltetrols and 3-MBTCA, which are oxidation products of isoprene and α-pinene, respectively.[1, 46-48] The temporal variation of 2-methyltetrols was similar to that of WSOC during the study period (R^2 = 0.47, P < 0.001). Moreover, the temporal variations of the concentrations of 3-MBTCA and WSOC were similar during the entire sampling period (R^2 = 0.74, P

197 < 0.001). These results indicated that most of the WSOC in the submicrometer aerosols
198 was associated with the emissions of isoprene and α-pinene and their oxidation at this
199 forest site.

200 The average concentration of sulfate in the submicrometer particles was 5.5 ± 3.1
201 μg m^{-3} during the study period. Regarding the possible sources of the observed sulfate,
202 the local wind data suggested that the observed sulfate was likely transported by the
203 surrounding urban area in both daytime and nighttime, as mentioned above (**Figure S1**).
204 Therefore, it is likely that anthropogenic sources dominantly contributed to the
205 observed sulfate at this forest site, which is also supported by the negligible contribution
206 of sea salt to the observed sulfate (0.1%) in this study. The major sources of sulfate
207 observed in Tokyo are attributable to manufacturing industries and energy production.[49]
208 The average concentration observed at the current forest site was larger than that (ave.
209 3.2 μg m^{-3}) reported for an urban area of Tokyo in summer.[29] The observed sulfate at
210 this forest site was likely more aged due to the transport from the urban area, which can
211 explain the difference in the concentration levels.

212 Overall, the temporal variation in the concentrations of WSON is similar to that
213 of sulfate, rather than WSOC (**Figures 1b** and **1d**). At some specific nights (e.g., July
214 31 to August 1 and August 7−8), WSON showed a significant increase in the
215 concentrations, which is contrary to the case of WSOC. This resulted in no significant
216 difference in the average concentration of WSON between daytime and nighttime
217 (**Table S1**). The WSON concentrations also showed a temporal trend similar to that of
218 ALW concentrations (**Figure 1d**). The similarity in the temporal variations suggests

219 that WSON formation is closely linked with ALW at this forest site.

220 In general, volatile species like ammonium are expected to be volatilized more
221 in daytime when ambient temperature was higher. In this study, the sampling duration
222 was set for 3 hours in daytime, partly in order to avoid volatilization of the aerosol
223 components within this shorter time of the sampling in daytime. However, ammonium,
224 which is one of the major volatile species in this study, systematically showed larger
225 concentrations in daytime than in nighttime. Moreover, the diurnal variations of
226 isoprene SOA and monoterpene SOA were similar to those of their precursor VOCs
227 obtained by in-situ measurements[34] during the entire period. Although the possibility of
228 volatilization loss during the sampling cannot be ruled out, it is expected that the
229 difference in the sampling time between daytime and nighttime did not significantly
230 affect our discussion.

231 **Potential Sources of ALW.** To investigate the potential sources of ALW in the
232 submicrometer aerosols, **Figure 2** investigates different outputs of the ALW
233 concentrations calculated by ISORROPIA-II to evaluate the contribution of sulfate and
234 nitrate to the ALW mass. The calculation showed insignificant difference (~5.4%) in
235 the ALW concentrations between the cases with and without an NH_4NO_3 input. In
236 contrast, the calculation without an $(NH_4)_2SO_4$ input resulted in a significant decrease
237 in the ALW concentrations compared to the base-case calculation. On average,
238 $(NH_4)_2SO_4$ contributed to 75% of the ALW mass at the forest site. The average fractions
239 of the ALW mass derived by $(NH_4)_2SO_4$ were similar during daytime (75%) and
240 nighttime (72%). The results quantitatively suggest that most of the ALW mass was

241 controlled by sulfate. Cheng et al.[50] suggested that SO_2 from anthropogenic sources can
242 be trapped by alkaline aerosol components such as ammonium in fine particles during
243 a haze event, followed by oxidation by NO_2 to form sulfate. This production mechanism
244 of sulfate might be self-amplified with an increase in ALW concentrations[50].

245 **Figure 2** also includes the ALW concentrations derived by organic matter. On
246 average, the mass concentrations of the ALW derived by organics were similar during
247 daytime (0.98 ± 0.35 μg m^{-3}) and nighttime (1.02 ± 0.43 μg m^{-3}). Organic components
248 in aerosols can promote or inhibit water uptake, which depends on the chemical
249 composition and relative abundance of organic matter as well as particle mixing
250 states.[51-56] In this study, the calculation assumed a hygroscopic parameter κ of 0.1 for
251 organic matter, which is a typical value for biogenic SOA.[33, 57, 58] The calculation
252 resulted in an insignificant increase (ave. 16%) in ALW concentration (**Figure 2**). The
253 ALW concentrations driven by organics were substantially lower than those derived by
254 $(NH_4)_2SO_4$ both in daytime and nighttime, suggesting that the contribution of organic
255 matter to the ALW mass was insignificant in this study. Insignificant contribution of
256 organics to the ALW mass was also suggested by a previous study, which predicted
257 ALW in the urban area of Tokyo.[29] The overall results suggest that the amount of ALW
258 in the submicrometer aerosol particles was mainly controlled by that of sulfate at this
259 forest site.

260 ALW mainly driven by anthropogenic sulfate has been reported by previous
261 studies.[27, 29, 45, 59] However, the current result differs from those obtained by Hodas et
262 al. in an agricultural region in Po Valley, Italy.[25] They suggested that anthropogenic

nitrate from local sources mainly controls the formation of ALW in $PM_{2.5}$. Indeed, the concentrations of nitrate reported by Hodas et al.[25] are much larger than the values presented in this study. Thus, the difference in the major contributor to ALW may be due to the differences in the relative abundance of the aerosol components (i.e., sulfate vs. nitrate) responsible for ALW, as also suggested by Hodas et al.[25] Moreover, it is expected that in regions with larger NO_x emission under the concentration levels of biogenic VOCs and sulfate similar to those in this study, the formation of ALW may be promoted.

Possible Sources of WSOC and WSON and their Linkages with ALW. While ISORROPIA-II was used to predict the ALW mass, a positive matrix factorization (PMF) analysis[60] was performed to apportion sources of the measured WSOC and WSON. The PMF resolved six interpretable factors, which were characterized by the enrichment of each tracer compound (**Figure S3**). **Figure 3** presents the contribution of each factor to the mass concentrations of WSOC, WSON, and ALW during daytime and nighttime. The PMF showed that, on average, most of the WSOC mass was attributable to biogenic sources both in daytime (86%) and nighttime (77%). Most of the biogenic sources are isoprene-SOA and α-pinene-SOA (F2 and F3), followed by PBAPs such as bacteria, fungi, and pollen (F4 and F5) (**Figures 3a** and **3d**). As shown previously, the mass concentrations of WSOC showed a distinct diurnal variation with a maximum in daytime. The overall result suggests that most of the WSOC mass was attributable to local biogenic sources. In contrast, anthropogenic sulfate-rich factor (F1) contributed small fractions of WSOC mass both in daytime (9.4%) and nighttime (19%), suggesting

that organic carbon from anthropogenic sources contributed to the small fraction of WSOC mass.

In contrast, the anthropogenic sulfate-rich factor (F1) contributed to 48% and 61% of WSON mass during the daytime and nighttime, respectively (**Figures 3b** and **3e**). In addition, the sum of the biogenic-SOA-relevant factors (F2 and F3) and the pollen-rich factor (F5) accounted for 51% (daytime) and 38% (nighttime) of WSON mass, which are also significant sources. The PMF showed that most of ALW concentrations were attributable to the anthropogenic sulfate-rich factor (F1) both in daytime (74%) and nighttime (83%), as shown in **Figures 3c** and **3f**. This result agrees with those derived by ISORROPIA-II, where $(NH_4)_2SO_4$ is a major factor controlling ALW mass in this study (**Figure 2**).

Figures 4a and **4b** show the concentrations of WSOC and WSON as functions of ALW concentrations. The WSOC concentrations tended to increase with increasing ALW concentrations. However, the concentrations of these two parameters showed less significant correlation coefficient ($R^2 < 0.1$) in this study. This result is different from that obtained by a recent study conducted in an agriculture area in Italy,[25] according to which the WSOC concentrations showed a significant positive correlation with ALW concentrations in $PM_{2.5}$. Their study implied that ALW promoted the formation of particulate WSOC in $PM_{2.5}$. The difference between the current study and Hodas et al.[25] may be due to the additional contributions of the other formation processes of WSOC in this study, such as gas-phase reactions of biogenic VOCs, and PBAPs (**Figures 3a** and **3d**), and/or the difference in the size cut of aerosol particles.

In contrast, the concentrations of WSON showed significant positive correlations with those of ALW both in daytime (R^2 = 0.41, P < 0.01) and nighttime (R^2 = 0.55, P < 0.01), as also expected from **Figure 1d**. The overall results suggest that the amount of ALW, mainly driven by anthropogenic sulfate, is significantly linked with WSON formation. Moreover, the mass ratio of WSON/WSOC showed significant correlations with ALW concentrations (**Figure 4c**), indicating that the increasing rate of the WSON mass was higher than that of WSOC with increasing mass of ALW.

Possible Formation Mechanisms of WSON. As shown in the previous section, the current result suggests that ALW, mainly driven by anthropogenic sulfate, significantly contributed to WSON formation at the forest site. One plausible mechanism for WSON formation is the aqueous-phase reactions of NH_3/NH_4^+ with biogenic organic carbon.[12] The formation of NOCs has been found in recent laboratory experiments as a result of reactive uptake of NH_3 by carbonyl species in aqueous-phase SOA.[12, 61, 62] More recently, Gen et al.[20] reported that NH_3/NH_4^+ in the aqueous phase can react with glyoxal monomers to form NOCs (e.g., imidazole, 2,2′-biimidazole, and imidazole-2-carboxaldehyde). In our current study, the concentrations of WSON indeed showed positive correlations with those of NH_4^+ (**Figure S5a**).

Gen et al.[20] also suggested that the formation rates of NOCs can be increased due to the “salting-in” effect caused by a large concentration of salts such as sulfate. In addition, it has also been reported that organic gas species have a stronger potential to be partitioned in the liquid phase compared to particle-phase organic matter.[26] It is thus likely that high abundance of ALW in this study promotes NOC formation. In the

present study, the WSON concentrations showed significant positive correlations with those of sulfate and ALW (**Figure S4**). The overall results support the idea that WSON formation from NH_4^+-related aqueous-phase reactions is promoted by the increased mass of ALW.

As shown in **Figure 3e**, the anthropogenic sulfate-rich factor (F1) contributed to the dominant source fraction of WSON, which was much larger in nighttime than in daytime. Moreover, the correlation coefficient between WSON and NH_4^+ in nighttime was larger than that in daytime (**Figure S5a**). This result also indicated that the aqueous-phase reactions of biogenic VOCs with NH_4^+ to form WSON were more important in nighttime at this forest site. In general, relatively high RH in nighttime leads to the phase partitioning of NH_3 into liquid phase, followed by a rapid equilibrium of NH_3 with the particle phase.[63] Previous laboratory studies suggested that chemical aging of biogenic SOA formed by ozonolysis of both α-pinene and limonene under the presence of NH_3/NH_4^+ can produce a significant amount of NOCs.[64-68] Such NOC formation associated with NH_3/NH_4^+ has been attributed to the mechanism of carbonyl-to-imine conversion.[64, 65, 68] In order to support the idea that NH_3/NH_4^+ efficiently reacted with biogenic VOCs to form WSON in our study, we compared the WSON and the product of ozone with α-pinene and limonene which were simultaneously measured at the sampling site. The results showed that the mass concentrations of WSON significantly correlated with the product of ozone with α-pinene and limonene particularly in nighttime with R^2 of 0.57and 0.49, respectively (**Figures S6a** and **S6b**). This result together with the PMF analysis provides evidence that aqueous-phase reactions of

NH_3/NH_4^+ with biogenic VOCs can partly explain the WSON formation in submicrometer particles at the forest site. Consequently, the increases in ALW concentrations in nighttime can serve as an abundant medium for NH_4^+-related aqueous reactions to form WSON.

Another possible mechanism is the formation of organic nitrate through reactions of biogenic VOCs and NO_x. Previous studies have suggested that NO_x oxidation of isoprene is closely related to the formation of MPAN, which can account for 8−13% of gas-phase organic nitrate.[69-71] These organic nitrates can be partitioned into the particle phase, followed by reactions in the aqueous phase.[14, 71, 72] In addition, particulate NOCs, including NOSs, dihydroxynitrates, and monohydroxynitrates, were found to be the reaction products of α-/β-pinene and NO_x.[14, 17] To support the reactions of biogenic VOCs with reactive nitrogen to form organic nitrate, **Figure 5** compares the concentrations of isoprene NOS identified by ESI/LC-MS and WSON during a specific period (July 31 to August 2, 2015) of this study. The concentrations of WSON showed a positive correlation with those of isoprene NOS, which is formed through the reactions of isoprene with NO_x and sulfate. Although this NOS is one example and it is difficult to cover all the molecular compounds of WSON, this result provides a direct evidence for WSON formation, partly by the reactions of biogenic VOCs and NO_x.

Production of organic nitrates in aerosols has been observed in nighttime at forest sites in northeastern Bavaria, Germany;[16] K-puszta, Hungary;[73] and Antwerp, Belgium.[74] These field studies suggest the importance of nitrate radical (NO_3)-driven chemistry in the formation of SOA. Such importance of NO_3 chemistry in nighttime

was also demonstrated by laboratory experiments, using sulfate seed aerosol under the conditions of both high and intermediate NO_x levels.[17] In this study, the observed concentration of NO_x was larger in nighttime (**Table S1**). Moreover, a positive correlation between the concentrations of WSON and the product of NO_x and O_3 ($[NO_x][O_3]$]) was evident only in nighttime ($P < 0.05$) (**Figure S6c**). The results indicate that the NO_x-related reactions were more important in the formation of WSON in nighttime than in daytime. It is noted that photosynthetically active radiation (PAR) as a surrogate of the sunlight did not show any significant correlations with ALW or NO_3^- ($R^2 < 0.1$) in this study (data not shown). This also supports that WSON and ALW is not a coincidence but are linked in terms of the formation of WSON.

Particle acidity is also an important factor affecting NO_x-involved chemistry to produce organic nitrates from isoprene and α-/β-pinene.[14, 22] In particular, particle acidity with pH < 2 can significantly influence the ring-opening reactions of isoprene epoxydiols.[22, 75] Indeed, the average pH values predicted by ISORROPIA-II in this study were as low as 1.18 ± 0.67 and 1.52 ± 0.50 in daytime and nighttime, respectively (**Table S1**). The high particle acidity supports the fact that the acid-catalyzed mechanism can also promote WSON formation from biogenic VOCs. This is in accordance with the conclusion of Miyazaki et al.,[1] who also indicated that a strong aerosol acidity can promote WSON formation.

Note that the pollen-rich factor (F5), which represents PBAPs, accounted for 18% of WSON in daytime (**Figure 3b**), whereas it was negligible in nighttime (<1.0%) (**Figure 3e**). Such PBAPs can contain amino acids, which are one of the most well-

known NOCs.[76, 77] While our study suggests the dominance of secondary processes in WSON formation in summer, similar studies need to be conducted in the other seasons, such as spring and autumn, when PBAP emissions are expected to be large.[33, 76]

In conclusion, our study suggests that ALW, mainly driven by local anthropogenic sulfate, significantly promoted WSON formation in submicrometer aerosol particles at this study site. Although it is difficult to quantitatively estimate the WSON mass increased by ALW only from our data, the coefficient of determination between WSON and ALW, at least showed that 41% (daytime) and 55% (nighttime) of the variability in the WSON mass concentrations can be explained by ALW. Aqueous-phase reactions involving ammonium and biogenic VOCs are likely important pathways for WSON formation. In addition, the interactions between biogenic VOCs and atmospheric reactive nitrogen also play a key role in WSON formation in aqueous-phase submicrometer particles, particularly in nighttime, at this forest site. These findings may provide not only new insights to the formation processes of WSON associated with ALW but also management strategies to control the abundance of submicrometer aerosol particles.

■ ASSOCIATED CONTENT

Supporting Information

Details of the calculation of ALW and pH, PMF analysis, one table (Table S1), and five extensive figures (Figures S1−S6) (PDF)

■ AUTHOR INFORMATION

Corresponding Authors

*Phone: +81-11-706-7448; e-mail: yuzom@lowtem.hokudai.ac.jp

ORCID

Yuzo Miyazaki: 0000-0001-9403-2772

Yu Xu: 0000-0001-8338-2283

Present Addresses

▽ (T.M.) School of Food and Nutritional Sciences, University of Shizuoka, Shizuoka 422-8526, Japan.

Notes

The authors declare no competing financial interest.

■ ACKNOWLEDGEMENTS

This research was supported in part by JSPS KAKENHI (grant numbers 16H02931 and 25281002) by the Ministry of Education, Culture, Sports, Science and Technology (MEXT) of Japan. The research is also funded by Steel Foundation for Environmental Protection Technology, Japan. Y. X. is an International Research Fellow of Japan Society for the Promotion of Science (Postdoctoral Fellowships for Research in Japan). We thank Hiroshi Tsurumaru, Kensuke Ito, and Tomihide Fujii for their help in the aerosol sampling and the gas measurements at the Field Museum Tama Hill measurement station of Tokyo University of Agriculture and Technology in 2015.

■ REFERENCES

(1) Miyazaki, Y.; Fu, P. Q.; Ono, K.; Tachibana, E.; Kawamura, K. Seasonal cycles of water-soluble organic nitrogen aerosols in a deciduous broadleaf forest in northern Japan. *J. Geophys. Res.: Atmos.* **2014,** *119* (3), 1440-1454.

(2) Zamora, L.; Prospero, J.; Hansell, D. A. Organic nitrogen in aerosols and

precipitation at Barbados and Miami: Implications regarding sources, transport and deposition to the western subtropical North Atlantic. *J. Geophys. Res.: Atmos.* **2011,** *116* (D20), D20309, doi: 20310.21029/22011JD015660.

(3) Cape, J. N.; Cornell, S. E.; Jickells, T. D.; Nemitz, E. Organic nitrogen in the atmosphere - Where does it come from? A review of sources and methods. *Atmos. Environ.* **2011,** *102* (1), 30-48.

(4) Jickells, T.; Baker, A.; Cape, J.; Cornell, S.; Nemitz, E. The cycling of organic nitrogen through the atmosphere. *Philos. T. R. Soc. B: Biol. Sci.* **2013,** *368* (1621), doi: 10.1098/rstb.2013.0115.

(5) Cornell, S. E. Atmospheric nitrogen deposition: Revisiting the question of the importance of the organic component. *Environ. Pollut.* **2011,** *159* (10), 2214-2222.

(6) Mace, K. A.; Artaxo, P.; Duce, R. A. Water-soluble organic nitrogen in Amazon Basin aerosols during the dry (biomass burning) and wet seasons. *J. Geophys. Res.: Atmos.* **2003,** *108* (D16), 4512. doi: 10.1029/2003JD003557.

(7) González Benítez, J. M.; Cape, J. N.; Heal, M. R.; van Dijk, N.; Díez, A. V. Atmospheric nitrogen deposition in south-east Scotland: Quantification of the organic nitrogen fraction in wet, dry and bulk deposition. *Atmos. Environ.* **2009,** *43* (26), 4087-4094.

(8) Altieri, K. E.; Fawcett, S. E.; Peters, A. J.; Sigman, D. M.; Hastings, M. G. Marine biogenic source of atmospheric organic nitrogen in the subtropical North Atlantic. *P. Natl. Acad. Sci. U. S. A.* **2016,** *113* (4), 925-930.

(9) Violaki, K.; Mihalopoulos, N. Water-soluble organic nitrogen (WSON) in size-

462 segregated atmospheric particles over the Eastern Mediterranean. *Atmos. Environ.* **2010,**
463 *44* (35), 4339-4345.
464 (10) Galloway, J. N.; Dentener, F. J.; Capone, D. G.; Boyer, E. W.; Howarth, R. W.;
465 Seitzinger, S. P.; Asner, G. P.; Cleveland, C.; Green, P.; Holland, E. Nitrogen cycles:
466 past, present, and future. *Biogeochemistry* **2004,** *70* (2), 153-226.
467 (11) Matos, J. T. V.; Duarte, R. M. B. O.; Duarte, A. C. Challenges in the identification
468 and characterization of free amino acids and proteinaceous compounds in atmospheric
469 aerosols: A critical review. *TrAC Trends Anal. Chem.* **2016,** *75*, 97-107.
470 (12) Montoya-Aguilera, J.; Hinks, M. L.; Aiona, P. K.; Wingen, L. M.; Horne, J. R.; Zhu,
471 S.; Dabdub, D.; Laskin, A.; Laskin, J.; Lin, P.; Nizkorodov, S. A., Reactive Uptake of
472 Ammonia by Biogenic and Anthropogenic Organic Aerosols. In *Multiphase*
473 *Environmental Chemistry in the Atmosphere*, American Chemical Society: 2018; Vol.
474 1299, pp 127-147.
475 (13) Perraud, V.; Bruns, E. A.; Ezell, M. J.; Johnson, S. N.; Yu, Y.; Alexander, M. L.;
476 Zelenyuk, A.; Imre, D.; Chang, W. L.; Dabdub, D. Nonequilibrium atmospheric
477 secondary organic aerosol formation and growth. *P. Natl. Acad. Sci. U. S. A.* **2012,** *109*
478 (8), 2836-2841.
479 (14) Hallquist, M.; Wenger, J. C.; Baltensperger, U.; Rudich, Y.; Simpson, D.; Claeys,
480 M.; Dommen, J.; Donahue, N.; George, C.; Goldstein, A. The formation, properties and
481 impact of secondary organic aerosol: current and emerging issues. *Atmos. Chem. Phys.*
482 **2009,** *9* (14), 5155-5236.
483 (15) Surratt, J. D.; Chan, A. W.; Eddingsaas, N. C.; Chan, M.; Loza, C. L.; Kwan, A. J.;

Hersey, S. P.; Flagan, R. C.; Wennberg, P. O.; Seinfeld, J. H. Reactive intermediates revealed in secondary organic aerosol formation from isoprene. *P. Natl. Acad. Sci. U. S. A.* **2010,** *107* (15), 6640-6645.

(16) Iinuma, Y.; Müller, C.; Berndt, T.; Böge, O.; Claeys, M.; Herrmann, H. Evidence for the existence of organosulfates from β-pinene ozonolysis in ambient secondary organic aerosol. *Environ. Sci. Technol.* **2007,** *41* (19), 6678-6683.

(17) Surratt, J. D.; Gómez-González, Y.; Chan, A. W.; Vermeylen, R.; Shahgholi, M.; Kleindienst, T. E.; Edney, E. O.; Offenberg, J. H.; Lewandowski, M.; Jaoui, M. Organosulfate formation in biogenic secondary organic aerosol. *J. Phys. Chem. A* **2008,** *112* (36), 8345-8378.

(18) Rollins, A. W.; Browne, E. C.; Min, K. E.; Pusede, S. E.; Wooldridge, P. J.; Gentner, D. R.; Goldstein, A. H.; Liu, S.; Day, D. A.; Russell, L. M. Evidence for NOx control over nighttime SOA formation. *Science* **2012,** *337* (6099), 1210-1212.

(19) Yu, G.; Bayer, A. R.; Galloway, M. M.; Korshavn, K. J.; Fry, C. G.; Keutsch, F. N. Glyoxal in aqueous ammonium sulfate solutions: products, kinetics and hydration effects. *Environ. Sci. Technol.* **2011,** *45* (15), 6336-6342.

(20) Gen, M.; Huang, D.; Chan, C. K. Reactive uptake of glyoxal by ammonium containing salt particles as a function of relative humidity. *Environ. Sci. Technol.* **2018,** *52* (12), 6903-6911.

(21) Faust, J. A.; Wong, J. P.; Lee, A. K.; Abbatt, J. P. Role of aerosol liquid water in secondary organic aerosol formation from volatile organic compounds. *Environ. Sci. Technol.* **2017,** *51* (3), 1405-1413.

(22) He, Q. F.; Ding, X.; Fu, X. X.; Zhang, Y. Q.; Wang, J. Q.; Liu, Y. X.; Tang, M. J.; Wang, X. M.; Rudich, Y. Secondary Organic Aerosol Formation from Isoprene Epoxides in the Pearl River Delta, South China: IEPOX- and HMML-Derived Tracers. *J. Geophys. Res.: Atmos.* **2018,** *123* (13), 6999-7012.

(23) Sareen, N.; Waxman, E. M.; Turpin, B. J.; Volkamer, R.; Carlton, A. G. Potential of aerosol liquid water to facilitate organic aerosol formation: assessing knowledge gaps about precursors and partitioning. *Environ. Sci. Technol.* **2017,** *51* (6), 3327-3335.

(24) Youn, J. S.; Wang, Z.; Wonaschütz, A.; Arellano, A.; Betterton, E. A.; Sorooshian, A. Evidence of aqueous secondary organic aerosol formation from biogenic emissions in the North American Sonoran Desert. *Geophys. Res. Lett.* **2013,** *40* (13), 3468-3472.

(25) Hodas, N.; Sullivan, A. P.; Skog, K.; Keutsch, F. N.; Collett Jr, J. L.; Decesari, S.; Facchini, M. C.; Carlton, A. G.; Laaksonen, A.; Turpin, B. J. Aerosol liquid water driven by anthropogenic nitrate: Implications for lifetimes of water-soluble organic gases and potential for secondary organic aerosol formation. *Environ. Sci. Technol.* **2014,** *48* (19), 11127-11136.

(26) Carlton, A.; Turpin, B. Particle partitioning potential of organic compounds is highest in the Eastern US and driven by anthropogenic water. *Atmos. Chem. Phys.* **2013,** *13* (20), 10203-10214.

(27) Guo, H. Y.; Xu, L.; Bougiatioti, A.; Cerully, K. M.; Capps, S. L.; Hite Jr, J.; Carlton, A.; Lee, S. H.; Bergin, M.; Ng, N. Fine-particle water and pH in the southeastern United States. *Atmos. Chem. Phys.* **2015,** *15* (9), 5211-5228.

(28) Xue, J.; Griffith, S. M.; Yu, X.; Lau, A. K. H.; Yu, J. Z. Effect of nitrate and sulfate

528 relative abundance in PM2.5 on liquid water content explored through half-hourly
529 observations of inorganic soluble aerosols at a polluted receptor site. *Atmos. Environ.*
530 **2014,** *99*, 24-31.
531 (29) Nguyen, T. K. V.; Zhang, Q.; Jimenez, J. L.; Pike, M.; Carlton, A. G. Liquid water:
532 ubiquitous contributor to aerosol mass. *Environ. Sci. Tech. Let.* **2016,** *3* (7), 257-263.
533 (30) Kanakidou, M.; Seinfeld, J.; Pandis, S.; Barnes, I.; Dentener, F.; Facchini, M.;
534 Dingenen, R. V.; Ervens, B.; Nenes, A.; Nielsen, C. Organic aerosol and global climate
535 modelling: a review. *Atmos. Chem. Phys.* **2005,** *5* (4), 1053-1123.
536 (31) Weber, R. J.; Sullivan, A. P.; Peltier, R. E.; Russell, A.; Yan, B.; Zheng, M.; De
537 Gouw, J.; Warneke, C.; Brock, C.; Holloway, J. S. A study of secondary organic aerosol
538 formation in the anthropogenic-influenced southeastern United States. *J. Geophys. Res.:*
539 *Atmos.* **2007,** *112* (D13), doi:10.1029/2007JD008408.
540 (32) Carlton, A. G.; Pye, H. O.; Baker, K. R.; Hennigan, C. J. Additional benefits of
541 federal air-quality rules: model estimates of controllable biogenic secondary organic
542 aerosol. *Environ. Sci. Technol.* **2018,** *52* (16), 9254-9265.
543 (33) Müller, A.; Miyazaki, Y.; Tachibana, E.; Kawamura, K.; Hiura, T. Evidence of a
544 reduction in cloud condensation nuclei activity of water-soluble aerosols caused by
545 biogenic emissions in a cool-temperate forest. *Sci. Rep.* **2017,** *7* (1), 8452.
546 doi:10.1038/s41598-017-08112-9.
547 (34) Nakayama, T.; Kuruma, Y.; Matsumi, Y.; Morino, Y.; Sato, K.; Tsurumaru, H.;
548 Ramasamy, S.; Sakamoto, Y.; Kato, S.; Miyazaki, Y. Missing ozone-induced potential
549 aerosol formation in a suburban deciduous forest. *Atmos. Environ.* **2017,** *171*, 91-97.

(35) Matsuda, K.; Watanabe, I.; Mizukami, K.; Ban, S.; Takahashi, A. Dry deposition of PM2.5 sulfate above a hilly forest using relaxed eddy accumulation. *Atmos. Environ.* **2015,** *107*, 255-261.

(36) Nakashima, Y.; Tsurumaru, H.; Sathiyamurthi, R.; Sakamoto, Y.; Kato, S.; Sadanaga, Y.; Nakayama, T.; Miyazaki, Y.; Mochiduki, T.; Wada, R.; Matsuda, K.; Kajii, Y. Ambient measurements and survey of the sources of gaseous glyoxal at suburban site in Tokyo during summer season. *Journal of Japan Society for Atmospheric Environment / Taiki Kankyo Gakkaishi* **2017,** *52* (6), 167-176.

(37) Miyazaki, Y.; Aggarwal, S. G.; Singh, K.; Gupta, P. K.; Kawamura, K. Dicarboxylic acids and water-soluble organic carbon in aerosols in New Delhi, India, in winter: Characteristics and formation processes. *J. Geophys. Res.: Atmos.* **2009,** *114* (D19), doi: 10.1029/2009JD011790.

(38) Miyazaki, Y.; Kawamura, K.; Jung, J.; Furutani, H.; Uematsu, M. Latitudinal distributions of organic nitrogen and organic carbon in marine aerosols over the western North Pacific. *Atmos. Chem. Phys.* **2011,** *11* (7), 3037-3049.

(39) Finessi, E.; Decesari, S.; Paglione, M.; Giulianelli, L.; Carbone, C.; Gilardoni, S.; Fuzzi, S.; Saarikoski, S.; Raatikainen, T.; Hillamo, R. Determination of the biogenic secondary organic aerosol fraction in the boreal forest by NMR spectroscopy. *Atmos. Chem. Phys.* **2012,** *12* (2), 941-959.

(40) Yttri, K. E.; Aas, W.; Bjerke, A.; Cape, J.; Cavalli, F.; Ceburnis, D.; Dye, C.; Emblico, L.; Facchini, M.; Forster, C. Elemental and organic carbon in PM 10: a one year measurement campaign within the European Monitoring and Evaluation

572 Programme EMEP. *Atmos. Chem. Phys.* **2007,** *7* (22), 5711-5725.
573 (41) Simon, H.; Bhave, P.; Swall, J.; Frank, N.; Malm, W. Determining the spatial and
574 seasonal variability in OM/OC ratios across the US using multiple regression. *Atmos.*
575 *Chem. Phys.* **2011,** *11* (6), 2933-2949.
576 (42) Nakayama, T.; Sato, K.; Tsuge, M.; Imamura, T.; Matsumi, Y. Complex refractive
577 index of secondary organic aerosol generated from isoprene/NOx photooxidation in the
578 presence and absence of SO2. *J. Geophys. Res.: Atmos.* **2015,** *120* (15), 7777-7787.
579 (43) Hettiyadura, A. P. S.; Jayarathne, T.; Baumann, K.; Goldstein, A. H.; de Gouw, J.
580 A.; Koss, A.; Keutsch, F. N.; Skog, K.; Stone, E. A. Qualitative and quantitative analysis
581 of atmospheric organosulfates in Centreville, Alabama. *Atmos. Chem. Phys.* **2017,** *17*
582 (2), 1343-1359.
583 (44) Bian, Y.; Zhao, C.; Ma, N.; Chen, J.; Xu, W. A study of aerosol liquid water content
584 based on hygroscopicity measurements at high relative humidity in the North China
585 Plain. *Atmos. Chem. Phys.* **2014,** *14* (12), 6417-6426.
586 (45) Nguyen, T.; Petters, M.; Suda, S.; Guo, H.; Weber, R.; Carlton, A. Trends in
587 particle-phase liquid water during the Southern Oxidant and Aerosol Study. *Atmos.*
588 *Chem. Phys.* **2014,** *14* (20), 10911-10930.
589 (46) Hu, Q. H.; Xie, Z. Q.; Wang, X. M.; Kang, H.; He, Q. F.; Zhang, P. F. Secondary
590 organic aerosols over oceans via oxidation of isoprene and monoterpenes from Arctic
591 to Antarctic. *Sci. Rep.* **2013,** *3*, 2280. DOI: 10.1038/srep02280.
592 (47) Claeys, M.; Szmigielski, R.; Kourtchev, I.; Van der Veken, P.; Vermeylen, R.;
593 Maenhaut, W.; Jaoui, M.; Kleindienst, T. E.; Lewandowski, M.; Offenberg, J. H.

Hydroxydicarboxylic acids: markers for secondary organic aerosol from the photooxidation of α-pinene. *Environ. Sci. Technol.* **2007,** *41* (5), 1628-1634.

(48) Claeys, M.; Graham, B.; Vas, G.; Wang, W.; Vermeylen, R.; Pashynska, V.; Cafmeyer, J.; Guyon, P.; Andreae, M. O.; Artaxo, P. Formation of secondary organic aerosols through photooxidation of isoprene. *Science* **2004,** *303* (5661), 1173-1176.

(49) Miyakawa, T.; Takegawa, N.; Kondo, Y. Removal of sulfur dioxide and formation of sulfate aerosol in Tokyo. *J. Geophys. Res.: Atmos.* **2007,** *112* (D13), doi: 10.1029/2006JD007896.

(50) Cheng, Y.; Zheng, G.; Wei, C.; Mu, Q.; Zheng, B.; Wang, Z.; Gao, M.; Zhang, Q.; He, K.; Carmichael, G. Reactive nitrogen chemistry in aerosol water as a source of sulfate during haze events in China. *Sci. Adv.* **2016,** *2* (12), e1601530. doi: 10.1126/sciadv.1601530.

(51) Lightstone, J. M.; Onasch, T. B.; Imre, D.; Oatis, S. Deliquescence, efflorescence, and water activity in ammonium nitrate and mixed ammonium nitrate/succinic acid microparticles. *J. Phys. Chem. A* **2000,** *104* (41), 9337-9346.

(52) Andrews, E.; Larson, S. M. Effect of surfactant layers on the size changes of aerosol particles as a function of relative humidity. *Environ. Sci. Technol.* **1993,** *27* (5), 857-865.

(53) Peng, C.; Chan, M. N.; Chan, C. K. The hygroscopic properties of dicarboxylic and multifunctional acids: Measurements and UNIFAC predictions. *Environ. Sci. Technol.* **2001,** *35* (22), 4495-4501.

(54) Choi, M. Y.; Chan, C. K. The effects of organic species on the hygroscopic

616 behaviors of inorganic aerosols. *Environ. Sci. Technol.* **2002,** *36* (11), 2422-2428.
617 (55) Chuang, P. Y. Measurement of the timescale of hygroscopic growth for atmospheric
618 aerosols. *J. Geophys. Res.: Atmos.* **2003,** *108* (D9), doi: 10.1029/2002JD002757.
619 (56) Medina, J.; Nenes, A. Effects of film-forming compounds on the growth of giant
620 cloud condensation nuclei: Implications for cloud microphysics and the aerosol indirect
621 effect. *J. Geophys. Res.: Atmos.* **2004,** *109* (D20), doi: 10.1029/2004JD004666.
622 (57) Gunthe, S.; King, S.; Rose, D.; Chen, Q.; Roldin, P.; Farmer, D.; Jimenez, J.; Artaxo,
623 P.; Andreae, M.; Martin, S. Cloud condensation nuclei in pristine tropical rainforest air
624 of Amazonia: size-resolved measurements and modeling of atmospheric aerosol
625 composition and CCN activity. *Atmos. Chem. Phys.* **2009,** *9* (19), 7551-7575.
626 (58) Dusek, U.; Frank, G.; Curtius, J.; Drewnick, F.; Schneider, J.; Kürten, A.; Rose, D.;
627 Andreae, M. O.; Borrmann, S.; Pöschl, U. Enhanced organic mass fraction and
628 decreased hygroscopicity of cloud condensation nuclei (CCN) during new particle
629 formation events. *Geophys. Res. Lett.* **2010,** *37* (3), doi: 10.1029/2009GL040930.
630 (59) Nguyen, T. K. V.; Capps, S. L.; Carlton, A. G. Decreasing Aerosol Water Is
631 Consistent with OC Trends in the Southeast U.S. *Environ. Sci. Technol.* **2015,** *49* (13),
632 7843-7850.
633 (60) Norris, G.; Duvall, R.; Brown, S.; Bai, S. EPA Positive Matrix Factorization (PMF)
634 5.0 fundamentals and User Guide Prepared for the US Environmental Protection
635 Agency Office of Research and Development. *Washington, DC.* **2014**.
636 (61) Kwon, D.; Or, V. W.; Sovers, M. J.; Tang, M.; Kleiber, P. D.; Grassian, V. H.; Young,
637 M. A. Optical Property Measurements and Single Particle Analysis of Secondary

638 Organic Aerosol Produced from the Aqueous-Phase Reaction of Ammonium Sulfate
639 with Methylglyoxal. *ACS Earth Space Chem.* **2018,** *2* (4), 356-365.
640 (62) Stangl, C. M.; Johnston, M. V. Aqueous Reaction of Dicarbonyls with Ammonia as
641 a Potential Source of Organic Nitrogen in Airborne Nanoparticles. *J. Phys. Chem. A*
642 **2017,** *121* (19), 3720-3727.
643 (63) Pan, Y.; Tian, S.; Liu, D.; Fang, Y.; Zhu, X.; Zhang, Q.; Zheng, B.; Michalski, G.;
644 Wang, Y. Fossil fuel combustion-related emissions dominate atmospheric ammonia
645 sources during severe haze episodes: Evidence from 15N-stable isotope in size-resolved
646 aerosol ammonium. *Environ. Sci. Technol.* **2016,** *50* (15), 8049-8056.
647 (64) Bones, D. L.; Henricksen, D. K.; Mang, S. A.; Gonsior, M.; Bateman, A. P.; Nguyen,
648 T. B.; Cooper, W. J.; Nizkorodov, S. A. Appearance of strong absorbers and
649 fluorophores in limonene-ozone secondary organic aerosol due to ammonium-
650 mediated chemical aging over long time scales. *J. Geophys. Res.: Atmos.* **2010,** *115*
651 (D5), D05203, doi:10.1029/2009JD012864.
652 (65) Laskin, J.; Laskin, A.; Roach, P. J.; Slysz, G. W.; Anderson, G. A.; Nizkorodov, S.
653 A.; Bones, D. L.; Nguyen, L. Q. High-resolution desorption electrospray ionization
654 mass spectrometry for chemical characterization of organic aerosols. *Anal. Chem.* **2010,**
655 *82* (5), 2048-2058.
656 (66) Nguyen, T. B.; Lee, P. B.; Updyke, K. M.; Bones, D. L.; Laskin, J.; Laskin, A.;
657 Nizkorodov, S. A. Formation of nitrogen-and sulfur-containing light-absorbing
658 compounds accelerated by evaporation of water from secondary organic aerosols. *J.*
659 *Geophys. Res.: Atmos.* **2012,** *117* (D1), doi: 10.1029/2011JD016944.

660 (67) Updyke, K. M.; Nguyen, T. B.; Nizkorodov, S. A. Formation of brown carbon via
661 reactions of ammonia with secondary organic aerosols from biogenic and
662 anthropogenic precursors. *Atmos. Environ.* **2012,** *63*, 22-31.
663 (68) Laskin, J.; Laskin, A.; Nizkorodov, S. A.; Roach, P.; Eckert, P.; Gilles, M. K.; Wang,
664 B.; Lee, H. J.; Hu, Q. Molecular selectivity of brown carbon chromophores. *Environ.*
665 *Sci. Technol.* **2014,** *48* (20), 12047-12055.
666 (69) Nguyen, T. B.; Laskin, J.; Laskin, A.; Nizkorodov, S. A. Nitrogen-containing
667 organic compounds and oligomers in secondary organic aerosol formed by
668 photooxidation of isoprene. *Environ. Sci. Technol.* **2011,** *45* (16), 6908-6918.
669 (70) Sprengnether, M.; Demerjian, K. L.; Donahue, N. M.; Anderson, J. G. Product
670 analysis of the OH oxidation of isoprene and 1, 3-butadiene in the presence of NO. *J.*
671 *Geophys. Res.: Atmos.* **2002,** *107* (D15), 4268. doi: 10.1029/2001JD000716.
672 (71) Paulot, F.; Crounse, J.; Kjaergaard, H.; Kroll, J.; Seinfeld, J.; Wennberg, P. Isoprene
673 photooxidation: new insights into the production of acids and organic nitrates. *Atmos.*
674 *Chem. Phys.* **2009,** *9* (4), 1479-1501.
675 (72) Pye, H. O.; Pinder, R. W.; Piletic, I. R.; Xie, Y.; Capps, S. L.; Lin, Y. H.; Surratt, J.
676 D.; Zhang, Z.; Gold, A.; Luecken, D. J. Epoxide pathways improve model predictions
677 of isoprene markers and reveal key role of acidity in aerosol formation. *Environ. Sci.*
678 *Technol.* **2013,** *47* (19), 11056-11064.
679 (73) Gómez-González, Y.; Surratt, J. D.; Cuyckens, F.; Szmigielski, R.; Vermeylen, R.;
680 Jaoui, M.; Lewandowski, M.; Offenberg, J. H.; Kleindienst, T. E.; Edney, E. O.
681 Characterization of organosulfates from the photooxidation of isoprene and unsaturated

682 fatty acids in ambient aerosol using liquid chromatography/(−) electrospray ionization
683 mass spectrometry. *J. Mass Spectrom.* **2008,** *43* (3), 371-382.
684 (74) Gómez-González, Y.; Wang, W.; Vermeylen, R.; Chi, X.; Neirynck, J.; Janssens, I.;
685 Maenhaut, W.; Claeys, M. Chemical characterisation of atmospheric aerosols during a
686 2007 summer field campaign at Brasschaat, Belgium: sources and source processes of
687 biogenic secondary organic aerosol. *Atmos. Chem. Phys.* **2012,** *12* (1), 125-138.
688 (75) Gaston, C. J.; Riedel, T. P.; Zhang, Z.; Gold, A.; Surratt, J. D.; Thornton, J. A.
689 Reactive uptake of an isoprene-derived epoxydiol to submicron aerosol particles.
690 *Environ. Sci. Technol.* **2014,** *48* (19), 11178-11186.
691 (76) Helin, A.; Sietiö, O. M.; Heinonsalo, J.; Bäck, J.; Riekkola, M. L.; Parshintsev, J.
692 Characterization of free amino acids, bacteria and fungi in size-segregated atmospheric
693 aerosols in boreal forest: seasonal patterns, abundances and size distributions. *Atmos.*
694 *Chem. Phys.* **2017,** *17* (21), 1-17.
695 (77) Xu, Y.; Wu, D. S.; Xiao, H. Y.; Zhou, J. X. Dissolved hydrolyzed amino acids in
696 precipitation in suburban Guiyang, southwestern China: Seasonal variations and
697 potential atmospheric processes. *Atmos. Environ.* **2019,** *211*, 247-255.
698
699

FIGURE CAPTIONS

Figure 1. Temporal variations in (a) the mass fractions of the chemical components in submicrometer water-soluble aerosols, mass concentrations of (b) WSOC, sulfate, and ammonium, (c) 2-methyltetrols and 3-MBTCA, and (d) WSON and ALW. Shaded areas in each panel indicate nighttime.

Figure 2. Temporal variations in the mass concentrations of ALW, compared to those without ammonium sulfate and ammonium nitrate, and those derived from organics calculated by ISORROPIA-II.

Figure 3. Contribution of each PMF-derived factor to the mass concentrations of (a) WSOC, (b) WSON, and (c) ALW during daytime and (d) WSOC, (e) WSON, and (f) ALW during nighttime.

Figure 4. Mass concentrations of (a) WSOC, (b) WSON, and (c) mass ratios of WSON to WSOC as a function of ALW concentrations during daytime (open circles) and nighttime (solid circles).

Figure 5. Scatter plot of mass concentrations of WSON and isoprene NOS with its chemical structure in submicrometer aerosol samples obtained during July 31 to August 2, 2015. Isoprene NOS is a molecular marker of isoprene-derived nitrooxy organosulfate detected at m/z 260 by ESI/LC-MS. Note that the chemical structure includes isomers of that compound.

Figures

Fig. 1.

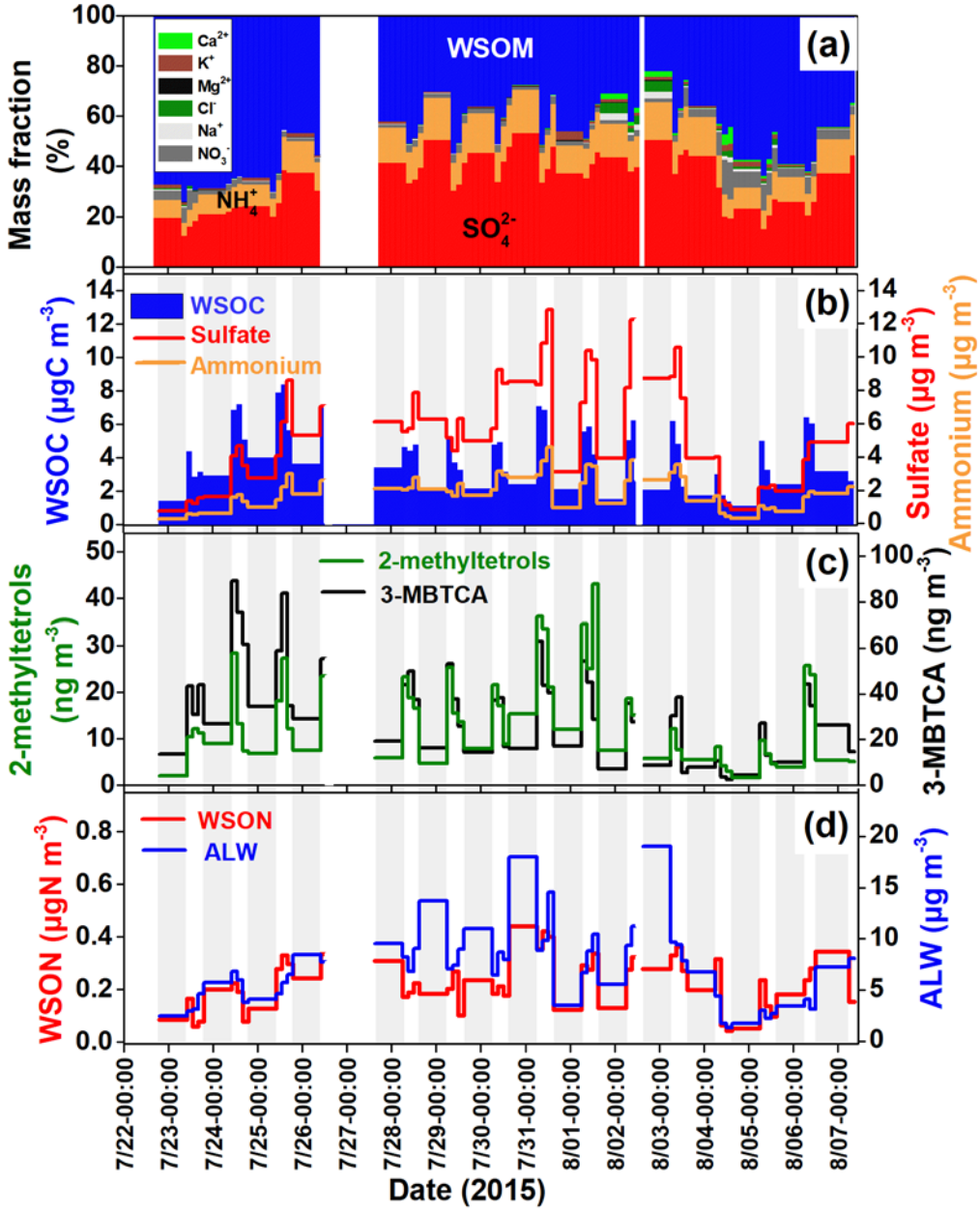

Fig. 2.

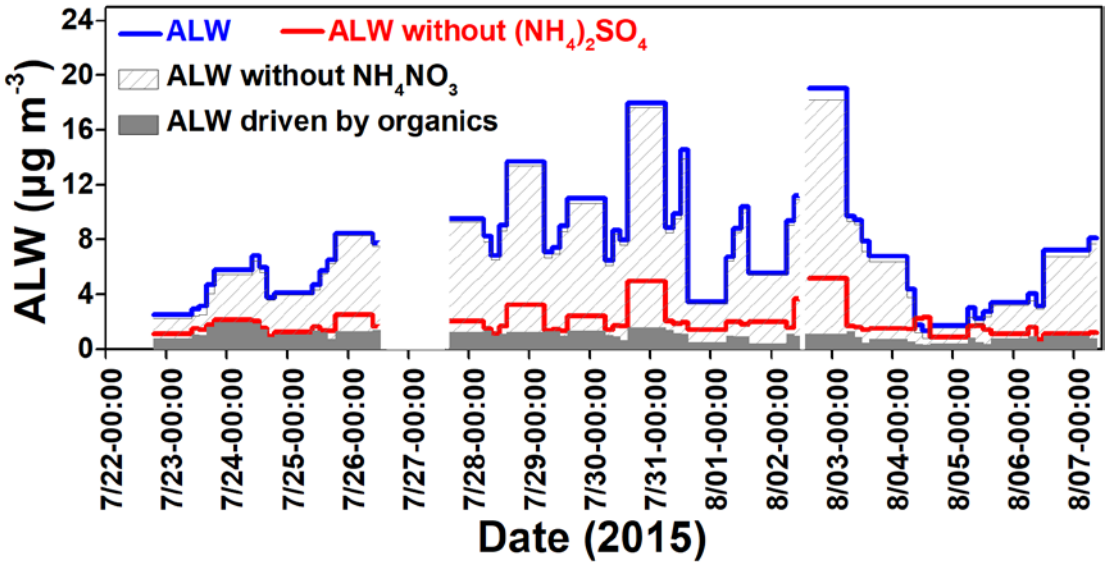
ALW
ALW without $(NH_4)_2SO_4$
ALW without NH_4NO_3
ALW driven by organics
ALW (μg m^{-3})
0
4
8
12
16
20
24
7/22-00:00
7/23-00:00
7/24-00:00
7/25-00:00
7/26-00:00
7/27-00:00
7/28-00:00
7/29-00:00
7/30-00:00
7/31-00:00
8/01-00:00
8/02-00:00
8/03-00:00
8/04-00:00
8/05-00:00
8/06-00:00
8/07-00:00
Date (2015)

Fig. 3.

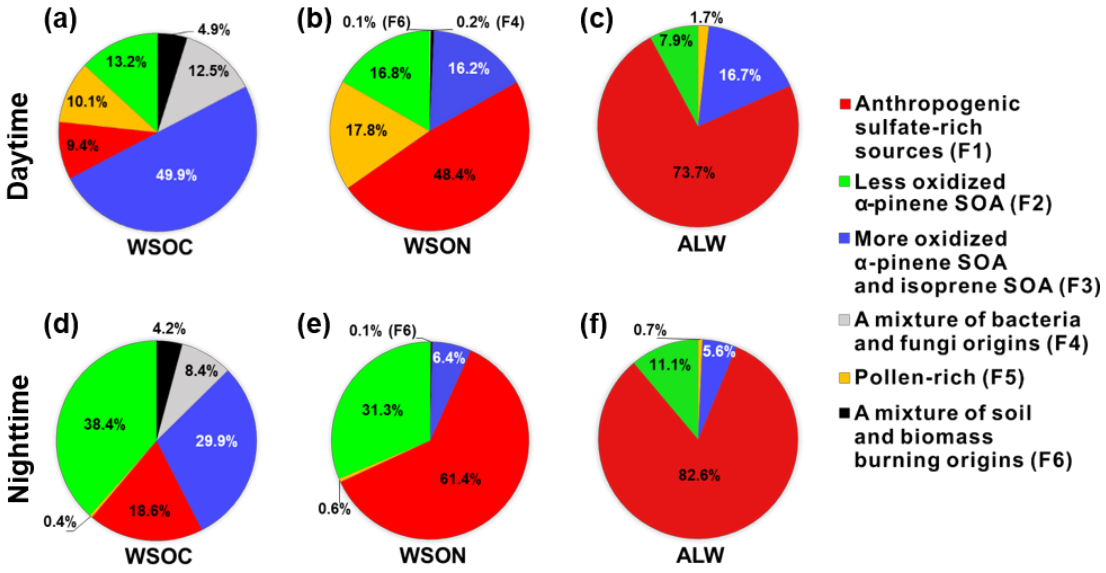
(a)
(b)
(c)
(d)
(e)
(f)
Daytime
Nighttime
WSOC
WSON
ALW
4.9%
12.5%
13.2%
10.1%
9.4%
49.9%
0.1% (F6)
0.2% (F4)
16.8%
16.2%
17.8%
48.4%
1.7%
7.9%
16.7%
73.7%
4.2%
8.4%
38.4%
29.9%
18.6%
0.4%
0.1% (F6)
6.4%
31.3%
61.4%
0.6%
0.7%
11.1%
5.6%
82.6%
Anthropogenic sulfate-rich sources (F1)
Less oxidized α-pinene SOA (F2)
More oxidized α-pinene SOA and isoprene SOA (F3)
A mixture of bacteria and fungi origins (F4)
Pollen-rich (F5)
A mixture of soil and biomass burning origins (F6)

768 **Fig. 4.**

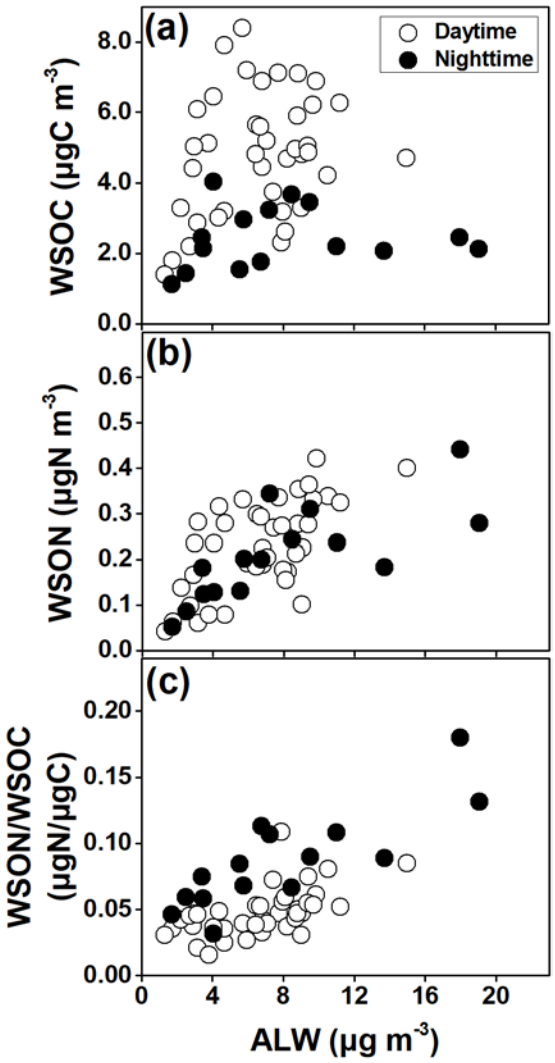
(a)
Daytime
Nighttime
WSOC (μgC m-3)
8.0
6.0
4.0
2.0
0.0
(b)
WSON (μgN m-3)
0.6
0.5
0.4
0.3
0.2
0.1
0.0
(c)
WSON/WSOC (μgN/μgC)
0.20
0.15
0.10
0.05
0.00
0
4
8
12
16
20
ALW (μg m-3)

769

Fig. 5.

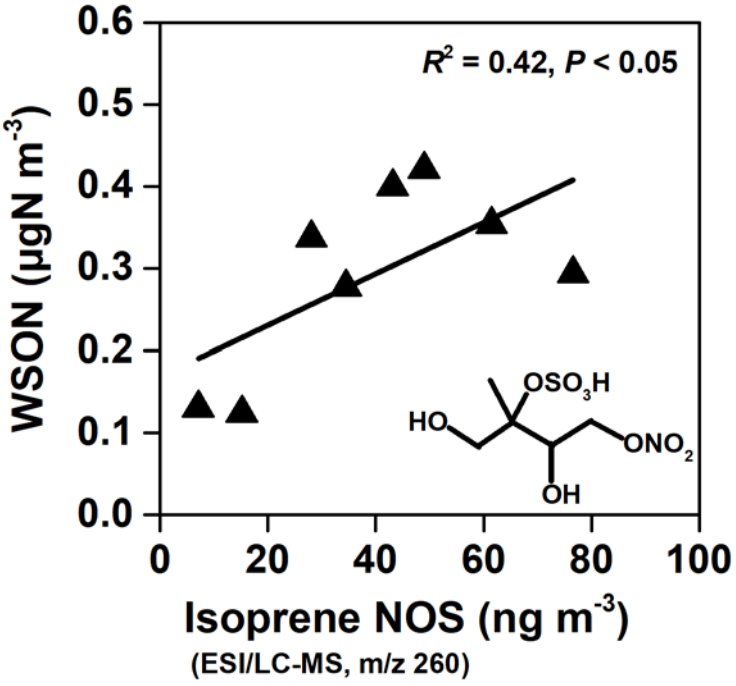
R^2 = 0.42, P < 0.05
WSON (µgN m^{-3})
0.0
0.1
0.2
0.3
0.4
0.5
0.6
0
20
40
60
80
100
Isoprene NOS (ng m^{-3})
(ESI/LC-MS, m/z 260)
HO
OSO$_3$H
ONO$_2$
OH

Aerosol liquid water promotes the formation of water-soluble organic nitrogen in submicrometer aerosols in a suburban forest

Yu Xu,[†] Yuzo Miyazaki,*[,†] Eri Tachibana,[†] Kei Sato,[‡] Sathiyamurthi Ramasamy,[‡, §] Tomoki Mochizuki,[†, ▽] Yasuhiro Sadanaga,[‖] Yoshihiro Nakashima,[⊥] Yosuke Sakamoto,[‡, §, #] Kazuhide Matsuda,[⊥] and Yoshizumi Kajii[‡, §, #]

[†]Institute of Low Temperature Science, Hokkaido University, Sapporo 060-0819, Japan

[‡]National Institute for Environmental Studies, Onogawa, Tsukuba, Ibaraki 305-5506, Japan

[§]Graduate School of Global Environmental Studies, Kyoto University, Nihonmatsucho, Sakyo-ku, Kyoto 606-8501, Japan

[‖]Department of Applied Chemistry, Osaka Prefecture University, Sakai 599-8531, Japan

[⊥]Department of Environmental Science on Biosphere, Tokyo University of Agriculture and Technology, Tokyo 183-8509, Japan

[#]Graduate School of Human and Environmental Studies, Kyoto University, Nihonmatsucho, Sakyo-ku, Kyoto 606-8501, Japan

[▽] Now at School of Food and Nutritional Sciences, University of Shizuoka, Shizuoka 422-8526, Japan.

*Corresponding author e-mail: yuzom@lowtem.hokudai.ac.jp

Phone: +81-11-706-7448

Address: Institute of Low Temperature Science, Hokkaido University, Sapporo 060-0819, Japan

Table of Contents

Aerosol Liquid Water (ALW) and pH Calculated by ISORROPIA-II

The mass concentrations of ALW associated with inorganic species were predicted by ISORROPIA-II.[1-3] This thermodynamic model also calculated the equilibrium particle hydronium ion concentration per volume air (H^+_{air}), which along with ALW was then used to predict particle pH.[1, 4] The calculation was based on concentrations of inorganic ions (Na^+, SO_4^{2-}, NH_4^+, NO_3^-, Cl^-, Ca^{2+}, K^+, and Mg^{2+}) measured by the ion chromatograph, as well as relative humidity (RH) and ambient temperature (T). In this study, ISORROPIA-II was run in the "reverse mode", which involves predicting the thermodynamic composition based only on the aerosol composition (i.e., without gas-phase parameters) together with RH and T as input. Moerover, the reverse mode with the thermodynamically metastable state was selected.[1, 2, 5]

Additionally, the "forward mode" was run with inputs of only aerosol-phase data, T, and RH. The resulting prediction of ALW concentration remained almost identical (reverse vs. forward: slope = 0.96, intercept: −0.2 μg m^{-3}, and r = 0.99) irrespective of the mode used. This is in agreement with the findings of Guo et al.[1] and Hennigan et al.[6]. When the ALW mass derived from organic matter accounts for less than 50% of the total ALW mass, the prediction of H^+_{air} by ISORROPIA-II is less sensitive to the amount of water derived by organics.[1] In such a case, ISORROPIA-II can calculate H^+_{air} without a large uncertainty even if the inputs are only inorganic species, T, and by the forward mode.[1, 4] Moreover, a previous study suggested that gas-phase input does not have an important impact on H^+_{air} calculation.[1, 4] Therefore, we also ran

ISORROPIA-II in the forward mode to estimate pH values of submicrometer aerosol particles.

The concentrations of ALW derived from organic compounds were estimated using a simplified model with the Zdanovskii−Stokes−Robinson (ZSR) mixing rule.[2] This rule shows that the hygroscopic growth of aerosol mixtures can be calculated using weighted hygroscopicity of each composition based on their dry volume fractions.[2, 7, 8] The ALW concentration derived from organic compounds was predicted according to the following equation:

$$V_{w,\,o} = V_o \kappa_{org} a_w / (1 - a_w) \quad (1)$$

where $V_{w,\,o}$ and V_o are volumes of ALW and organic components, respectively. κ_{org} represents the hygroscopicity parameter for organics, and a_w is water activity. For the calculation, the a_w value is considered equal to ambient RH based on the assumption that the effect of aerosol curvature is limited and that the effect of aerosol water uptake on ambient vapor pressure can be ignored.[7] In addition, the typical values of 1.4 g cm^{-3} and 0.1 were used for the density of organics and κ_{org}, respectively.[9-16]

The total concentration of ALW from inorganic and organic fractions was calculated using the aerosol inorganic–organic mixture functional group activity coefficient (AIOMFAC) model.[17] Hodas et al.[17] suggested that organic compounds that are not measured in aerosols may change aerosol hygroscopicity, resulting in over- or under-estimates of the ALW concentrations. Consequently, the κ-Kohler theory with the ZSR mixing rule has been generally accepted as a reliable method for predicting ALW concentration from the organic fraction in aerosols.[2, 7, 8]

Positive Matrix Factorization (PMF) Analysis.

The PMF version 5.0 (PMF 5.0)[18] was applied to develop source apportionments of WSOC, WSON, and ALW in submicrometer aerosol particles. Sixteen chemical components were used as the model inputs, including 2-methyltetrols, pinic acid, 3-methyl-1,2,3-butanetricarboxylic acid (3-MBTCA), arabitol, mannitol, trehalose, sucrose, ammonium, sulfate, calcium, potassium, nitrate, EC, ALW, WSON, and WSOC.

We ran the PMF model with 4−9 factors and changed the seed value from 1 to 40. Moreover, we examined the Q(robust) and Q(true) values as well as the number of scaled residuals beyond three standard deviations to select the optimal number of factors. The uncertainties of the PMF solutions for each test run were estimated using the analyses of displacement (DISP) and bootstrap (BS).[19, 20]

The PMF analysis resulted in six interpretable factors, as shown in Figure S3. Factor 1 (F1) was dominated by sulfate (85%) and ammonium (79%). As stated in the main text and shown in Figure S1, the local wind data suggest that the forest site was influenced by anthropogenic air masses transported from the urban area in the south, as well as by local biogenic sources, particularly in daytime. Therefore, F1 is referred to as “anthropogenic sulfate-rich sources.” Factor 2 (F2) is characterized by the dominance of pinic acid, which is the first-generation oxidation product of α-pinene.[21, 22] Thus, F2 is referred to here as “less oxidized α-pinene SOA.”

Factor 3 (F3) is characterized by large contributions of 3-MBTCA (67%) and 2-methyltetrols (58%). This profile can be explained by the dominant contributions of

both more oxidized α-pinene SOA and isoprene SOA.[22-24] F3 is defined as "more oxidized α-pinene SOA and isoprene SOA." Note that 54% of nitrate and 49% of EC also contributed to this factor. While the observed concentrations of nitrate and EC were relatively low (Table S1), the result implies that anthropogenic sources also contributed to F3 to some extent, and that NO_x was likely involved in the reactions with biogenic VOCs (see text).

Factor 4 (F4) is characterized by arabitol (81%), mannitol (86%), and trehalose (82%), whereas Factor 5 (F5) is dominated by sucrose (84%). On the basis of the characteristics of each source profile, F4 and F5 are referred to here as "a mixture of bacteria and fungi origins"[19, 25] and "pollen-rich"[19], respectively. Factor 6 (F6) is dominated by nss-Ca^{2+} (91%) and K^+ (75%). Moreover, there were some contributions of three sugar compounds, such as trehalose, to F6. Based on these characteristics, F6 is referred to here as "a mixture of soil and biomass burning origins".

Table S1. The minimum, maximum, and mean values of the major parameters observed and predicted in daytime and nighttime.

	Daytime			Nighttime		
	Min.	Max.	Mean ± SD	Min.	Max.	Mean ± SD
WSON (μgN m^{-3})	0.04	0.42	0.23 ± 0.10	0.05	0.44	0.21 ± 0.10
WSOC (μgC m^{-3})	1.40	8.39	4.84 ± 1.72	1.12	4.03	2.44 ± 0.83
SO_4^{2-} (μg m^{-3})	1.09	12.84	6.02 ± 3.19	0.75	8.70	4.24 ± 2.42
NO_3^- (μg m^{-3})	0.39	1.46	0.65 ± 0.26	0.12	0.50	0.21 ± 0.09
NH_4^+ (μg m^{-3})	0.44	4.57	2.16 ± 1.04	0.27	2.77	1.41 ± 0.76
2-methyltetrols (ng m^{-3})	2.90	43.07	16.92 ± 9.62	1.60	15.28	6.70 ± 3.40
3-MBTCA (ng m^{-3})	2.55	89.11	38.23 ± 20.33	4.41	34.35	16.80 ± 8.64
Pinonic acid (PNA) (ng m^{-3})	0.36	29.59	9.52 ± 5.87	1.12	3.81	2.06 ± 0.78
Pinic acid (PA) (ng m^{-3})	0.11	9.41	2.70 ± 2.28	0.78	4.98	2.45 ± 1.25
Arabitol (ng m^{-3})	0.04	7.81	2.94 ± 1.86	0.42	3.88	1.14 ± 0.93
Mannitol (ng m^{-3})	0.28	20.99	7.73 ± 5.64	0.80	8.15	2.56 ± 2.02
Sucrose (ng m^{-3})	0.07	21.35	4.38 ± 4.62	0.04	2.08	0.48 ± 0.60
Trehalose (ng m^{-3})	0.07	9.31	3.33 ± 2.47	0.34	8.63	1.82 ± 2.11
EC (μgC m^{-3})	BDL[a]	0.22	0.13 ± 0.08	0.10	0.18	0.16 ± 0.04
NO_2 (ppbv)	1.42	5.90	3.57 ± 1.27	5.48	10.67	8.30 ± 1.59
NO (ppbv)	BDL[a]	0.98	0.44 ± 0.36	0.50	2.45	1.07 ± 0.63
O_3 (ppbv)	19.85	104.96	64.79 ± 23.32	5.57	49.34	21.28 ± 11.24
Temperature (℃)	27.00	34.85	30.63 ± 1.58	25.81	28.13	26.79 ± 0.77
RH (%)	40.14	79.85	60.80 ± 6.99	63.83	83.62	75.38 ± 6.37
Inorganic ALW (μg m^{-3})	1.01	13.46	5.69 ± 2.82	1.33	17.97	7.00 ± 5.00
Organic ALW (μg m^{-3})	0.31	1.85	0.98 ± 0.35	0.39	1.96	1.02 ± 0.43
Total ALW (μg m^{-3})	1.32	14.96	6.68 ± 2.96	1.72	19.05	8.01 ± 5.20
pH	0.09	3.51	1.18 ± 0.67	0.26	1.90	1.52 ± 0.50

a BDL indicates value is below detection limit

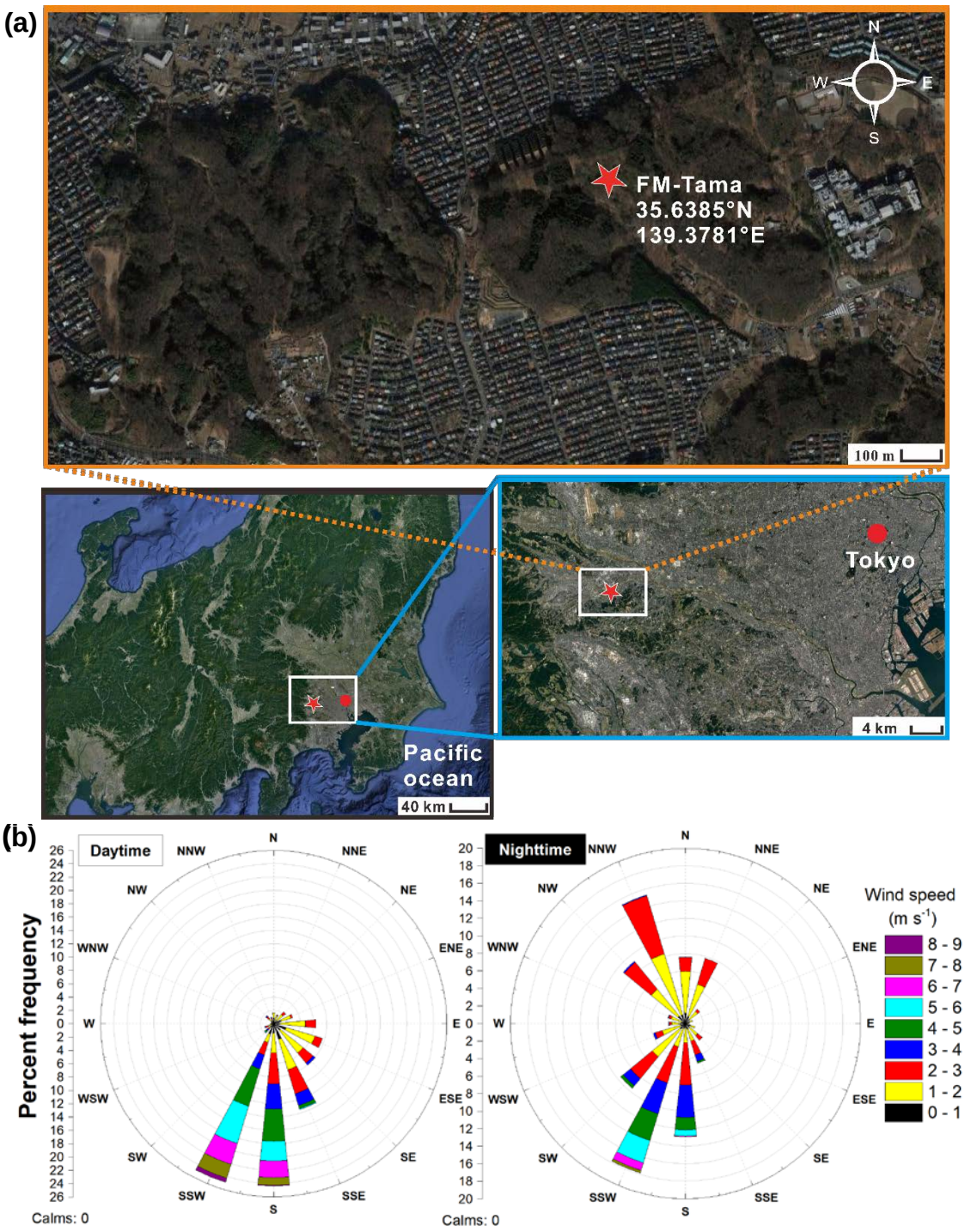

Figure S1. (a) The location of the sampling site. The observed frequencies of the local wind directions with wind speeds in (a) daytime and (b) nighttime.

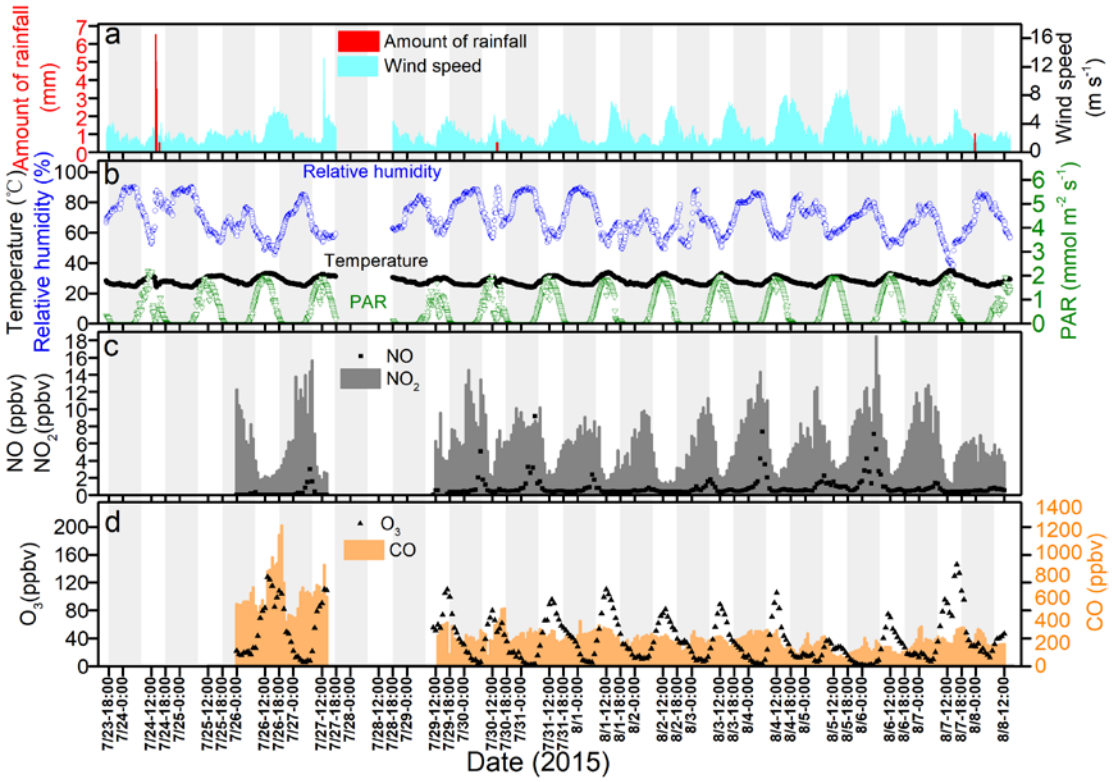

153

154 **Figure S2.** Temporal variations in (a) amount of rainfall and wind speed, (b)

155 temperature, relative humidity, and photosynthetically active radiation (PAR), (c) NO

156 and NO_2 mixing ratios, and (d) O_3 and CO mixing ratios at the aerosol sampling site.

157 Shaded areas in each panel indicate the nighttime.

158

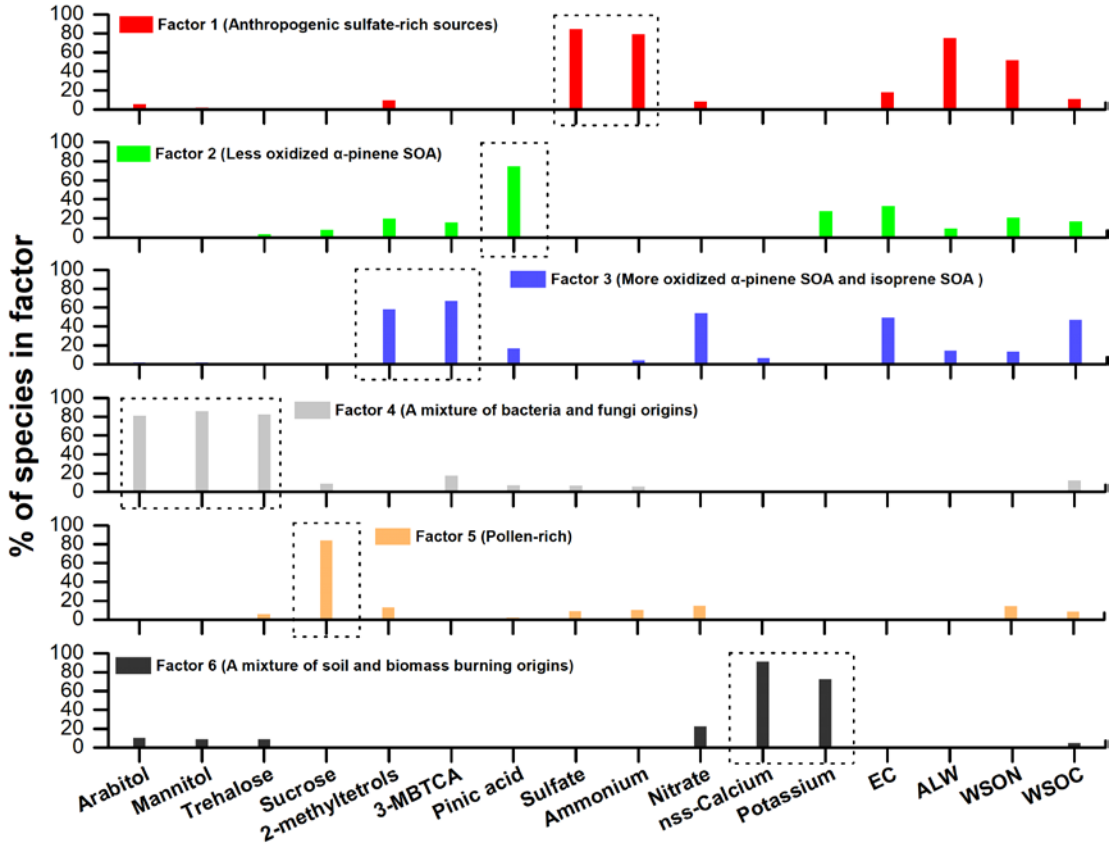

Figure S3. Six factor profiles derived from the PMF solution. The percentage of chemical species in each factor is shown.

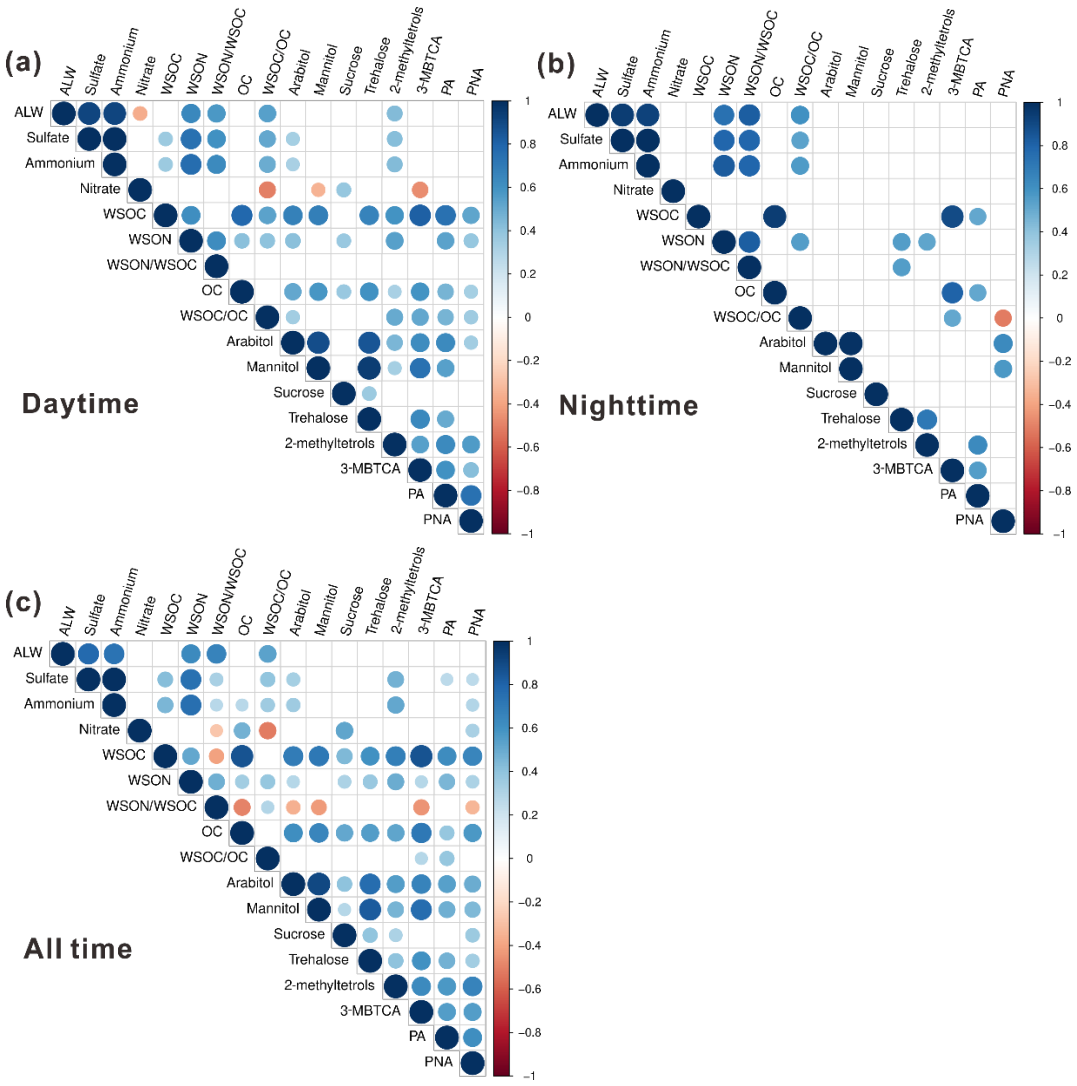

Figure S4. Diagrams presenting Spearman correlations among the parameters in the submicrometer aerosols for (a) daytime, (b) nighttime, and (c) all the data. The color of a solid circle denotes a correlation coefficient value *r*. The size of the solid circle indicates a significance of the correlation between the two corresponding parameters: the larger circle indicates that the correlation is more significant, whereas the smallest circle indicates *P*-value less than 0.05.

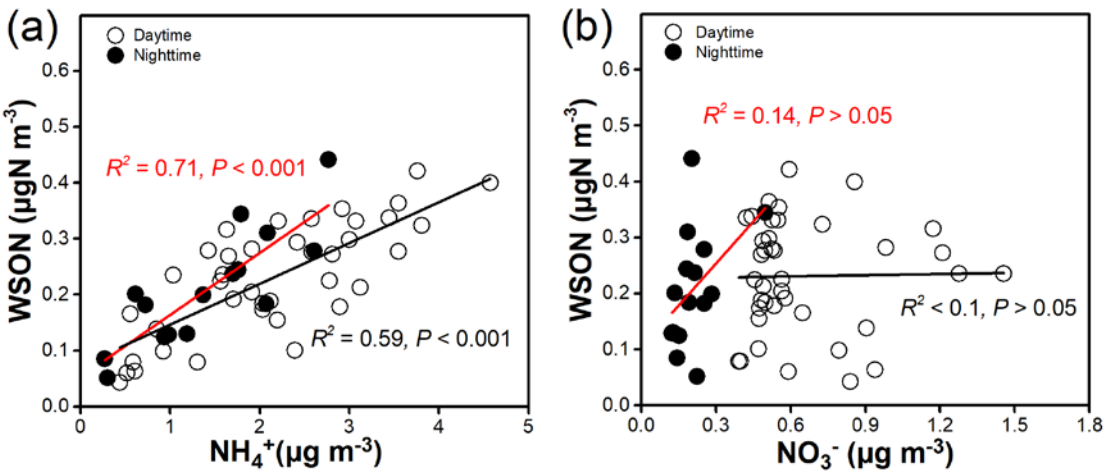

Figure S5. Scatterplots of the mass concentrations of WSON with those of (a) NH_4^+ and (b) NO_3^-. Black and red lines show regression lines in daytime and nighttime, respectively.

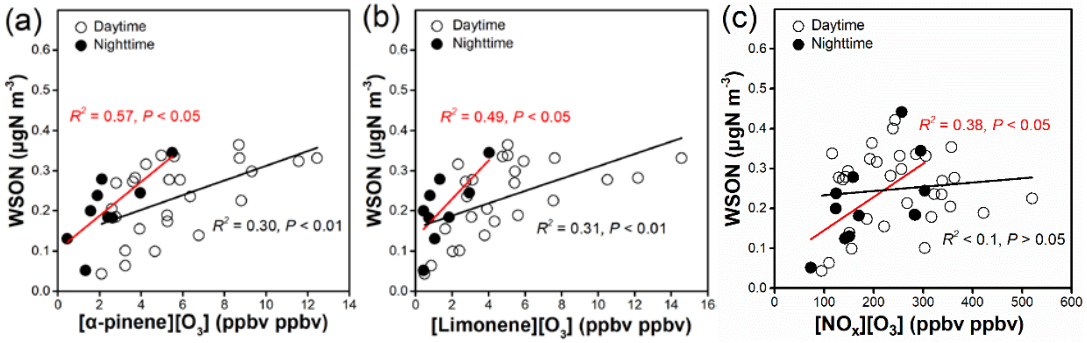

Figure S6. The mass concentrations of WSON as functions of the products by O_3 with (a) α-pinene ([α-pinene][O_3]), (b) limonene ([limonene][O_3]), and (c) NO_x ([NO_x][O_3]). Black and red lines show regression lines in daytime and nighttime, respectively.

REFERENCES.

(1) Guo, H. Y.; Xu, L.; Bougiatioti, A.; Cerully, K. M.; Capps, S. L.; Hite Jr, J.; Carlton, A.; Lee, S. H.; Bergin, M.; Ng, N. Fine-particle water and pH in the southeastern United States. *Atmos. Chem. Phys.* **2015,** *15* (9), 5211-5228.

(2) Nguyen, T. K. V.; Zhang, Q.; Jimenez, J. L.; Pike, M.; Carlton, A. G. Liquid water: ubiquitous contributor to aerosol mass. *Environ. Sci. Tech. Let.* **2016,** *3* (7), 257-263.

(3) Tan, H.; Cai, M.; Fan, Q.; Liu, L.; Li, F.; Chan, P. W.; Deng, X.; Wu, D. An analysis of aerosol liquid water content and related impact factors in Pearl River Delta. *Sci. Total Environ.* **2017,** *579*, 1822-1830.

(4) He, Q. F.; Ding, X.; Fu, X. X.; Zhang, Y. Q.; Wang, J. Q.; Liu, Y. X.; Tang, M. J.; Wang, X. M.; Rudich, Y. Secondary Organic Aerosol Formation from Isoprene Epoxides in the Pearl River Delta, South China: IEPOX- and HMML-Derived Tracers. *J. Geophys. Res.: Atmos.* **2018,** *123* (13), 6999-7012.

(5) Nguyen, T. K. V.; Capps, S. L.; Carlton, A. G. Decreasing Aerosol Water Is Consistent with OC Trends in the Southeast U.S. *Environ. Sci. Technol.* **2015,** *49* (13), 7843-7850.

(6) Hennigan, C.; Izumi, J.; Sullivan, A.; Weber, R.; Nenes, A. A critical evaluation of proxy methods used to estimate the acidity of atmospheric particles. *Atmos. Chem. Phys.* **2015,** *15* (5), 2775-2790.

(7) Bian, Y.; Zhao, C.; Ma, N.; Chen, J.; Xu, W. A study of aerosol liquid water content based on hygroscopicity measurements at high relative humidity in the North China Plain. *Atmos. Chem. Phys.* **2014,** *14* (12), 6417-6426.

(8) Nguyen, T.; Petters, M.; Suda, S.; Guo, H.; Weber, R.; Carlton, A. Trends in particle-phase liquid water during the Southern Oxidant and Aerosol Study. *Atmos. Chem. Phys.* **2014,** *14* (20), 10911-10930.

(9) King, S. M.; Rosenoern, T.; Shilling, J. E.; Chen, Q.; Martin, S. T. Cloud condensation nucleus activity of secondary organic aerosol particles mixed with sulfate. *Geophys. Res. Lett.* **2007,** *34* (24), doi: 10.1029/2007GL030390.

(10) Engelhart, G.; Asa-Awuku, A.; Nenes, A.; Pandis, S. CCN activity and droplet growth kinetics of fresh and aged monoterpene secondary organic aerosol. *Atmos. Chem. Phys.* **2008,** *8* (14), 3937-3949.

(11) Kuwata, M.; Zorn, S. R.; Martin, S. T. Using elemental ratios to predict the density of organic material composed of carbon, hydrogen, and oxygen. *Environ. Sci. Technol.* **2011,** *46* (2), 787-794.

(12) Cerully, K.; Bougiatioti, A.; Hite Jr, J.; Guo, H.; Xu, L.; Ng, N.; Weber, R.; Nenes, A. On the link between hygroscopicity, volatility, and oxidation state of ambient and water-soluble aerosols in the southeastern United States. *Atmos. Chem. Phys.* **2015,** *15* (15), 8679-8694.

(13) Prenni, A. J.; Petters, M. D.; Kreidenweis, S. M.; DeMott, P. J.; Ziemann, P. J. Cloud droplet activation of secondary organic aerosol. *J. Geophys. Res.: Atmos.* **2007,** *112* (D10), doi: 10.1029/2006JD007963.

(14) Wex, H.; Petters, M.; Carrico, C.; Hallbauer, E.; Massling, A.; McMeeking, G.; Poulain, L.; Wu, Z.; Kreidenweis, S.; Stratmann, F. Towards closing the gap between hygroscopic growth and activation for secondary organic aerosol: Part 1–Evidence from

measurements. *Atmos. Chem. Phys.* **2009,** *9* (12), 3987-3997.

(15) Dusek, U.; Frank, G.; Curtius, J.; Drewnick, F.; Schneider, J.; Kürten, A.; Rose, D.; Andreae, M. O.; Borrmann, S.; Pöschl, U. Enhanced organic mass fraction and decreased hygroscopicity of cloud condensation nuclei (CCN) during new particle formation events. *Geophys. Res. Lett.* **2010,** *37* (3), doi: 10.1029/2009GL040930.

(16) Gunthe, S.; King, S.; Rose, D.; Chen, Q.; Roldin, P.; Farmer, D.; Jimenez, J.; Artaxo, P.; Andreae, M.; Martin, S. Cloud condensation nuclei in pristine tropical rainforest air of Amazonia: size-resolved measurements and modeling of atmospheric aerosol composition and CCN activity. *Atmos. Chem. Phys.* **2009,** *9* (19), 7551-7575.

(17) Hodas, N.; Sullivan, A. P.; Skog, K.; Keutsch, F. N.; Collett Jr, J. L.; Decesari, S.; Facchini, M. C.; Carlton, A. G.; Laaksonen, A.; Turpin, B. J. Aerosol liquid water driven by anthropogenic nitrate: Implications for lifetimes of water-soluble organic gases and potential for secondary organic aerosol formation. *Environ. Sci. Technol.* **2014,** *48* (19), 11127-11136.

(18) Norris, G.; Duvall, R.; Brown, S.; Bai, S. EPA Positive Matrix Factorization (PMF) 5.0 fundamentals and User Guide Prepared for the US Environmental Protection Agency Office of Research and Development. *Washington, DC.* **2014**.

(19) Müller, A.; Miyazaki, Y.; Tachibana, E.; Kawamura, K.; Hiura, T. Evidence of a reduction in cloud condensation nuclei activity of water-soluble aerosols caused by biogenic emissions in a cool-temperate forest. *Sci. Rep.* **2017,** *7* (1), 8452. doi:10.1038/s41598-017-08112-9.

(20) Brown, S. G.; Eberly, S.; Paatero, P.; Norris, G. A. Methods for estimating

255 uncertainty in PMF solutions: Examples with ambient air and water quality data and
256 guidance on reporting PMF results. *Sci. Total Environ.* **2015,** *518*, 626-635.
257 (21) Szmigielski, R.; Surratt, J. D.; Gómez-González, Y.; Van der Veken, P.; Kourtchev,
258 I.; Vermeylen, R.; Blockhuys, F.; Jaoui, M.; Kleindienst, T. E.; Lewandowski, M. 3-
259 methyl-1, 2, 3-butanetricarboxylic acid: An atmospheric tracer for terpene secondary
260 organic aerosol. *Geophys. Res. Lett.* **2007,** *34* (24), doi: 10.1029/2007GL031338.
261 (22) Hu, Q. H.; Xie, Z. Q.; Wang, X. M.; Kang, H.; He, Q. F.; Zhang, P. F. Secondary
262 organic aerosols over oceans via oxidation of isoprene and monoterpenes from Arctic
263 to Antarctic. *Sci. Rep.* **2013,** *3*, 2280. DOI: 10.1038/srep02280.
264 (23) Miyazaki, Y.; Fu, P. Q.; Ono, K.; Tachibana, E.; Kawamura, K. Seasonal cycles of
265 water-soluble organic nitrogen aerosols in a deciduous broadleaf forest in northern
266 Japan. *J. Geophys. Res.: Atmos.* **2014,** *119* (3), 1440-1454.
267 (24) Claeys, M.; Graham, B.; Vas, G.; Wang, W.; Vermeylen, R.; Pashynska, V.;
268 Cafmeyer, J.; Guyon, P.; Andreae, M. O.; Artaxo, P. Formation of secondary organic
269 aerosols through photooxidation of isoprene. *Science* **2004,** *303* (5661), 1173-1176.
270 (25) Simoneit, B. R.; Elias, V. O.; Kobayashi, M.; Kawamura, K.; Rushdi, A. I.;
271 Medeiros, P. M.; Rogge, W. F.; Didyk, B. M. Sugars dominant water-soluble organic
272 compounds in soils and characterization as tracers in atmospheric particulate matter.
273 *Environ. Sci. Technol.* **2004,** *38* (22), 5939-5949.
274